Report Number: FEP-02-10

ANALYSIS OF HIGH PERFORMANCE CONCRETE SECTIONS ALONG I-90 NEAR TOMAH, WISCONSIN

FINAL REPORT

June 2010

FINAL REPORT

For the

ANALYSIS OF HIGH PERFORMANCE CONCRETE PAVEMENT SECTIONS ALONG I-90 NEAR TOMAH, WISCONSIN

WisDOT Report FEP-02-10

Wisconsin Highway Research Study # WI-01-08
"HIGH PERFORMANCE CONCRETE PAVEMENT"

Presented To:
Wisconsin Department of Transportation
Division of Transportation System Development
Bureau of Technical Services
3502 Kinsman Blvd.
Madison, WI 53704

Submitted By:

James A. Crovetti

June 2010

WisDOT Contact Peter Kemp

Technical Report Documentation Page

1. Report No. FEP 02-10	2. Government Accession No	3. Recipient's Catalog No
4. Title and Subtitle Analysis of High Performance Concrete Pavement Sections Along I-90 Near Tomah, Wisconsin		5. Report Date June 2010 6. Performing Organization Code WI-01-08
7. Authors James A. Crovetti	WisDOT Contact Peter Kemp	8. Performing Organization Report No. FEP-02-10
9. Performing Organization Name and Address James A Crovetti 4986 Arthur Road Slinger, WI 53086		10. Work Unit No. (TRAIS) 11. Contract or Grant No.
12. Sponsoring Agency Name and Address Wisconsin Department of Transportation Division of Transportation System Development Bureau of Technical Services 3502 Kinsman Blvd Madison, WI 53704		13. Type of Report and Period Covered Final Report, Sep 2008 – June 2010

15. Supplementary Notes

16. Abstract

This report presents the analysis of the High Performance Concrete (HPC) pavement sections constructed along the eastbound lanes of Interstate 90 near Tomah, Wisconsin. The test sections are the first specific HPC pavements designed and built in the State of Wisconsin and represent the current trends in building highway pavements with significantly longer service lives. Deflection data obtained with the WisDOT Falling Weight Deflectometer (FWD) was used to characterize the pavement materials within each section and to provide inputs for detailed mechanistic-empirical pavement analyses. The FWD data analysis indicated general uniformity within each constructed section, in terms of the concrete slab elastic modulus and foundation support k-value. The doweled transverse contraction joints within each test section are providing adequate load transfer, with measure deflection load transfers in excess of 90% for all sections. The deflection load transfer measured across the longitudinal joint separating the driving lane and the tied-concrete shoulder was adequate within TS1 (90%) but significantly reduced within TS2 (35%).

The Mechanistic Empirical Pavement Design Guide (MEPDG) software was used to provide 60-year predictions of pavement performance within each test section. The results indicate all sections should remain below a threshold value of 0.25 inches of transverse joint faulting throughout this period. Furthermore, no slab cracking is predicted within the HPC test sections 1 and 2; however, approximately 25% slab cracking is predicted within the control section (TS3). This increased slab cracking is above the threshold value of 15% slab cracking but below the terminal value of 50% slab cracking. The MEPDG software predicts 60-year IRI values above the threshold value of 180 inches per mile for all test sections. This result is predominantly due to predictions of high levels of joint spalling, which may be biasing the results.

17. Key Words High Performance Concrete Pavement, Falling Weight Deflectometer, Finite Element Analysis, Mechanistic-Empirical Pavement Design	18. Distribution Statement No restriction. This document is available to the public through the National Technical Information Service,5285 Port Royal Road, Springfield VA 22161

19. Security Classif.(of this report) Unclassified	19. Security Classif. (of this page) Unclassified	20. No. of Pages 40	21. Price

Form DOT F 1700.7 (8-72) Reproduction of completed page authorized

DISCLAIMER

This research was funded by the Wisconsin Department of Transportation and the Federal Highway Administration under Project # FEP-01-08. The contents of this report reflect the views of the author who is responsible for the facts and the accuracy of the data presented herein. The contents do not necessarily reflect the official views of the Wisconsin Department of Transportation or the Federal Highway Administration at the time of publication.

This document is disseminated under the sponsorship of the Wisconsin Department of Transportation in the interest of information exchange. The United States Government assumes no liability for its contents or use thereof. This report does not constitute a standard, specification or regulation.

The United States Government does not endorse products or manufacturers. Trade and manufacturers' names appear in this report only because they are considered essential to the object of the document.

ACKNOWLEDGEMENTS

The author greatly appreciates the support, advice, and technical contributions received from Mr. Peter Kemp of the Wisconsin Department of Transportation.

TABLE OF CONTENTS

INTRODUCTION ……1

ANALYSIS OF FWD TESTING DATA ……2

Pre-Paving FWD Testing – Sept 17,2002 ……..…….2

Pre-Paving FWD Testing – Sept 18,2002 ……..…….8

Post-Construction FWD Testing – October 18, 2002 …….13

Post-Construction FWD Testing – November 8, 2002 …….15

Post-Construction FWD Testing – April 17-18, 2007 ……15

ANALYSIS OF PROJECTED PAVEMENT PERFORMANCE ……20

MEPDG v 1.0 Performance Analysis ……20

FINITE ELEMENT ANALYSIS ……30

MECHANISTIC ANALYSIS …….37

SUMMARY AND RECOMMENDATIONS …….40

INTRODUCTION

This report presents the analysis of the High Performance Concrete (HPC) pavement sections constructed along the eastbound lanes of Interstate 90 near Sparta, Wisconsin. The test sections are the first specific HPC pavements designed and built in the State of Wisconsin and represent the current trends in building highway pavements with significantly longer service lives.

The HPC pavement sections are located on I-90 in Monroe County immediately west of the intersection with STH 16, approximately 8 miles west of the I90-94 split in Tomah. These sections were designed to provide a 50-year service life with no planned maintenance during this period. WisDOT Report # WI-03-04 details the construction of the HPC sections. The specifics of each test section and the control section are as follows:

Test Section 1 – Station 2003+50 to 2010+95
Two 12 foot travel lanes
Tied 6 inch concrete shoulders (4 ft left and 10 ft right)
13.5 inch plain jointed concrete pavement (JPCP)
15 ft transverse joints perpendicular to traffic
Stainless steel dowels, 1.5 inch dia., 18 inches long, 12 inch c-c spacing
4 inch open graded No. 2 base course
4 inch dense graded base course – 1.5 inch maximum aggregate size
6 inch dense graded base course – 3 inch maximum aggregate size
16 inch breaker run subbase

Test Section 2 – Station 2010+95 to 2018+90
Two 12 foot travel lanes
Tied 6 inch concrete shoulders (4 ft left and 10 ft right)
13.5 inch plain jointed concrete pavement (JPCP)
15 ft transverse joints perpendicular to traffic
Stainless steel dowels, 1.5 inch dia., 18 inches long, 12 inch c-c spacing
Stainless steel tie bars across shoulder joints
4 inch open graded No. 2 base course
6 inch dense graded base course

Test Section 3 (Control) – Station 2018+90 to 2026+00
Two 12 foot travel lanes
3 inch HMA shoulders (4 ft left and 10 ft right)
12.25 inch plain jointed concrete pavement (JPCP)
15 ft transverse joints perpendicular to traffic
Standard epoxy coated steel dowels, 1.5 inch dia., 18 inches long, 12 inch c-c spacing
4 inch open graded No. 2 base course
6 inch dense graded base course

2.0 Analysis of FWD Testing Data

Deflection testing was conducted by WisDOT during four separate test periods, including 1) prior to placement of dense graded aggregate base materials, 2) one month after placement of the PCC surface, 3) two months after placement of the PCC surface, and 4) 4.5 years after opening to traffic.

2.1 Pre-Paving FWD Testing – Sept 17, 2002

Initial FWD testing was conducted within the limits of Test Sections 1 & 2 (TS1, TS2) on September 17, 2002. Tests were conducted within TS1 both before and after placement of the breaker run layer. Tests were conducted within TS2 on the graded soils, before compaction and placement of the dense graded aggregate layer.

Before placement tests in TS1 were limited to a 100-ft section between stations 2010+00 to 2011+00. The FWD was positioned within the right wheel path of the driving lane (DL-RWP), the center of the driving lane (DL-CEN), and the center of the passing lane (PL-CEN). Tests were conducted using FWD loads ranging from approximately 3,000 to 13,000 lbs. Deflection data was used to estimate the subgrade modulus based on the following:

$$Esg = \frac{0.081P}{\delta_0} \qquad (1)$$

$$Esg = \frac{0.2792P}{\delta_i r_i} \qquad (2)$$

Where: Esg = subgrade modulus, ksi
P = FWD load, lbs
δ_0 = maximum deflection, mils
δ_i = deflection at i inches from load center, mils
r_i = distance from load center, inches

Equation 2 was applied to data obtained from sensor readings out to a distance of 24 inches from the center of loading. The effective subgrade modulus at each test location was estimated as the minimum value obtained by the application of Eqns. 1 & 2. Figures 1 through 3 provide profile plots of effective subgrade moduli for each test load. As shown, there is a general tendency of increased subgrade modulus with increasing load level, most likely the result of increase densification under loading combined with the general tendency of stress-stiffening granular materials. Figure 4 provides a summary profile of the effective subgrade moduli computed based on the second drop at approximately 3,000 lbs. This minimum loading was chosen to represent the stress state after placement of the completed pavement structure. As shown, there is generally uniformity within each line of testing, with the centerline of the driving lane (DL-CEN) exhibiting comparatively higher values.

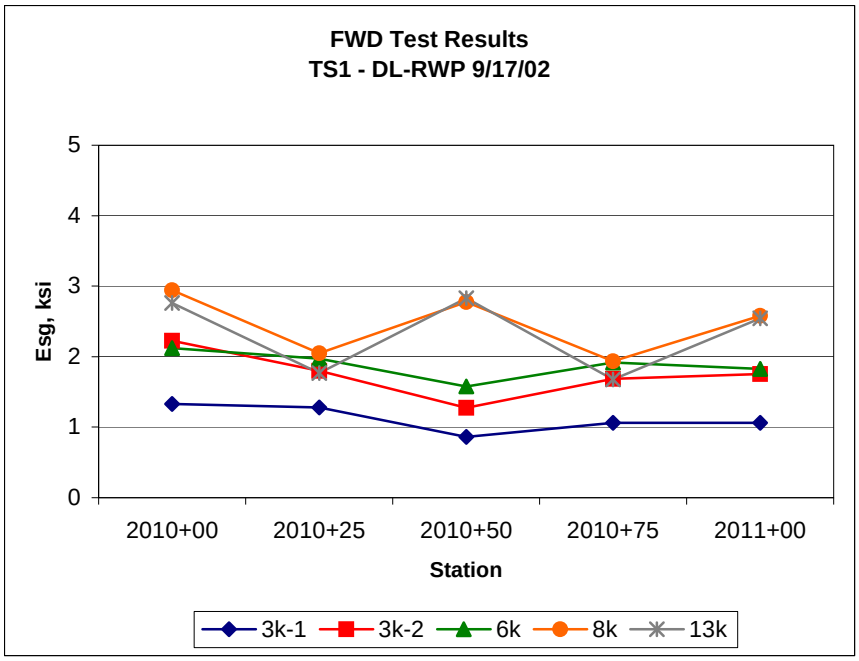

Figure 1: Effective Subgrade Moduli from Wheelpath Testing in Driving Lane

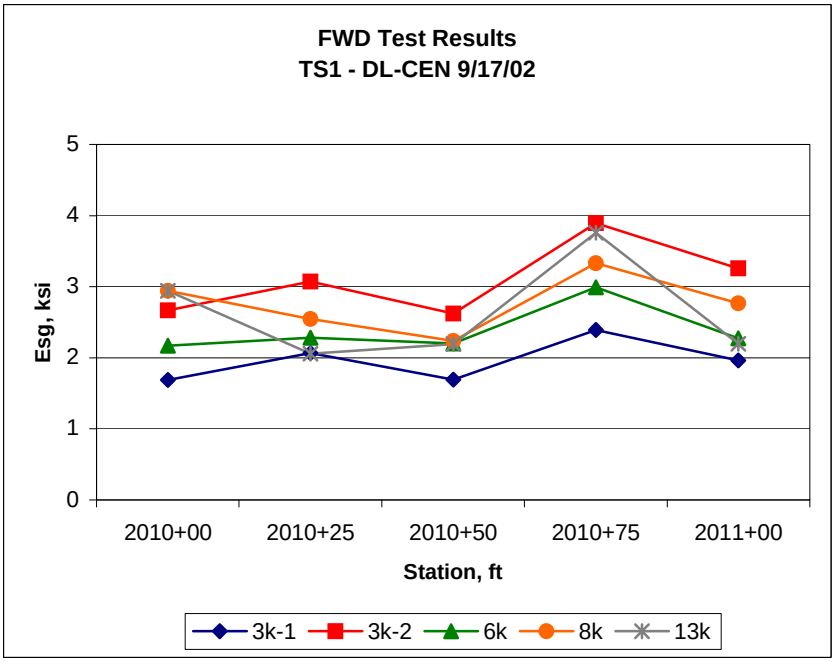

Figure 2: Effective Subgrade Moduli from Center Lane Testing in Driving Lane

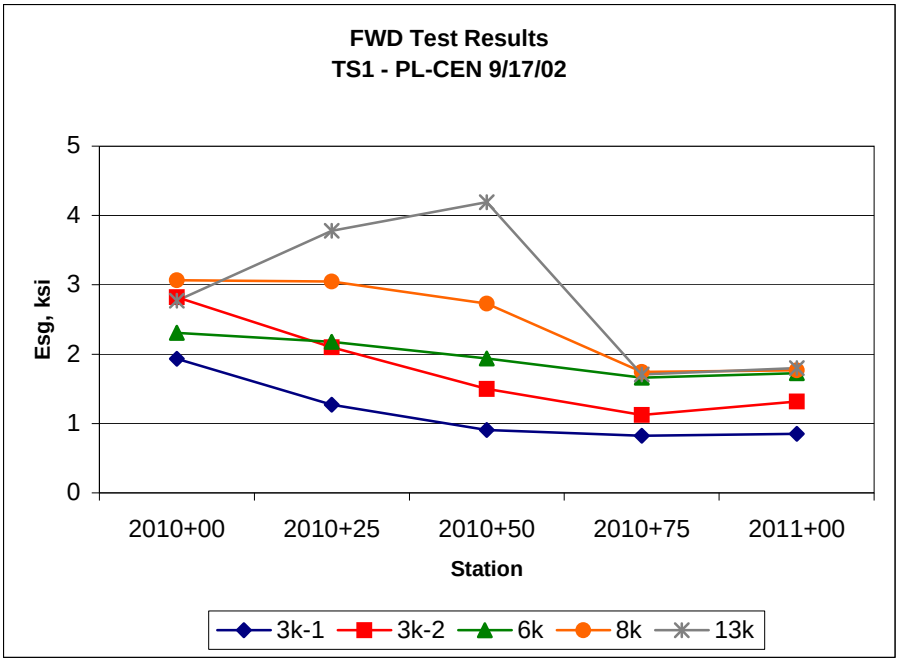

Figure 3: Effective Subgrade Moduli from Center Lane Testing in Passing Lane

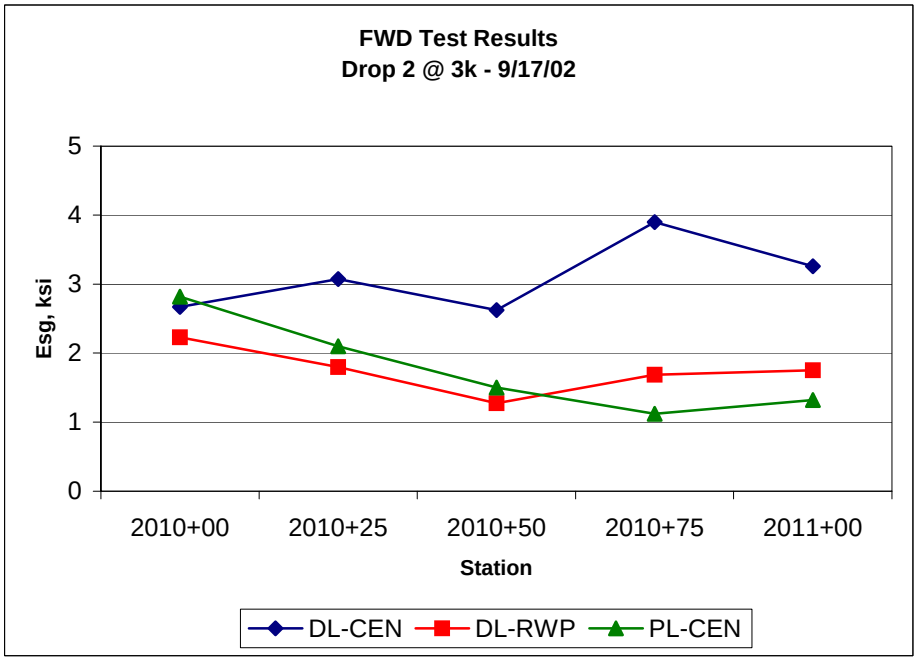

Figure 4: Effective Subgrade Moduli from 3kip Load Drop

Additional FWD tests were conducted in TS1 between stations 2005+00 to 2009+00 after breaker run placement. The FWD was positioned only within the right wheel path of the driving lane (DL-RWP) using FWD loads ranging from approximately 3,000 to 12,000 lbs. The effective subgrade modulus at each test location was estimated as the minimum value obtained by the application of Eqn. 2.2. Figure 2.5 provides profile plots of the effective subgrade moduli for each test load. As shown, there is a general tendency of decreased subgrade modulus with increasing load level, which is the general tendency of stress-softening fine-grained materials. The effective modulus of the breaker run layer was estimated by the following:

$$F_2 = \frac{12.37\delta_0 E_{sg}}{P} \tag{3}$$

$$E_{brkr} = E_{sg} 0.428 F_2^{-2.409} \tag{4}$$

Where: F_2 = 2-layer deflection factor
E_{brkr} = Effective modulus of the breaker run, ksi

Equation 4 was developed based on an assumption of an 16-inch thickness of breaker run materials. Figure 6 provides profile plots of the effective breaker moduli for each test load. As shown, there is great scatter in the data with a general tendency of increased breaker modulus with increasing load level, which is the general tendency of stress-stiffening granular materials. Figure 7 provides a re-scaled profile plot of the breaker modulus, focused on the predominant values which are well below 100 ksi.

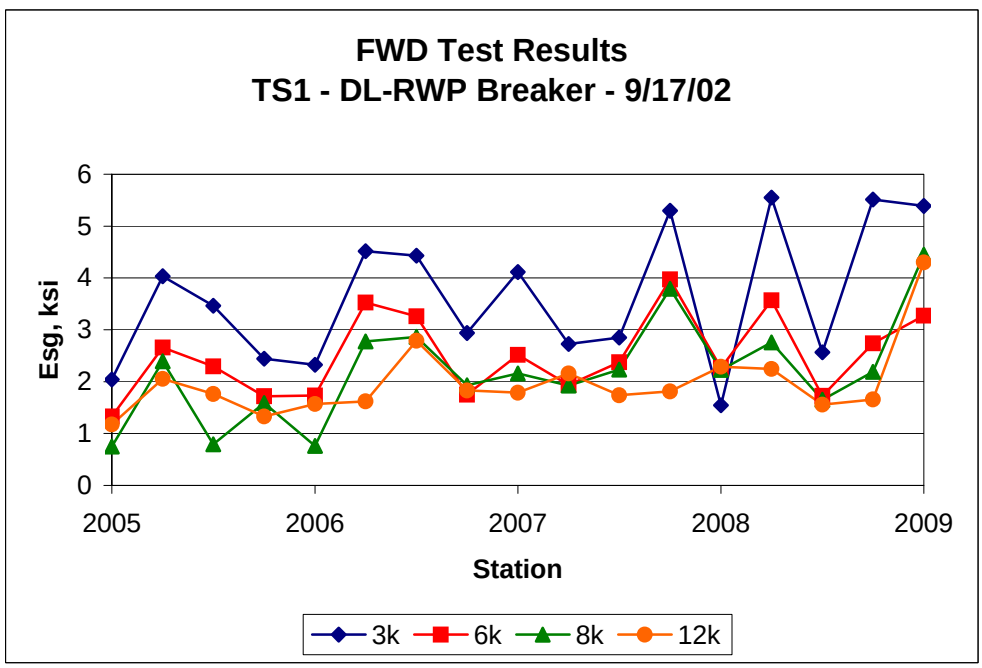

Figure 5: Effective Subgrade Moduli After Breaker Run Placement

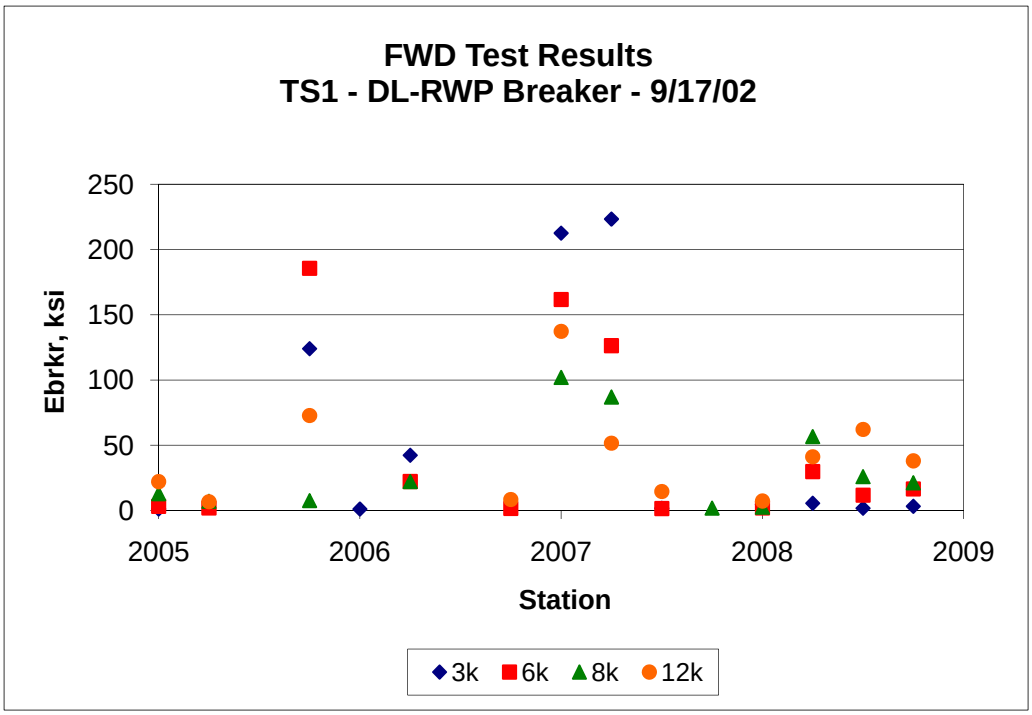

Figure 6: Effective Moduli of Breaker Run Layer

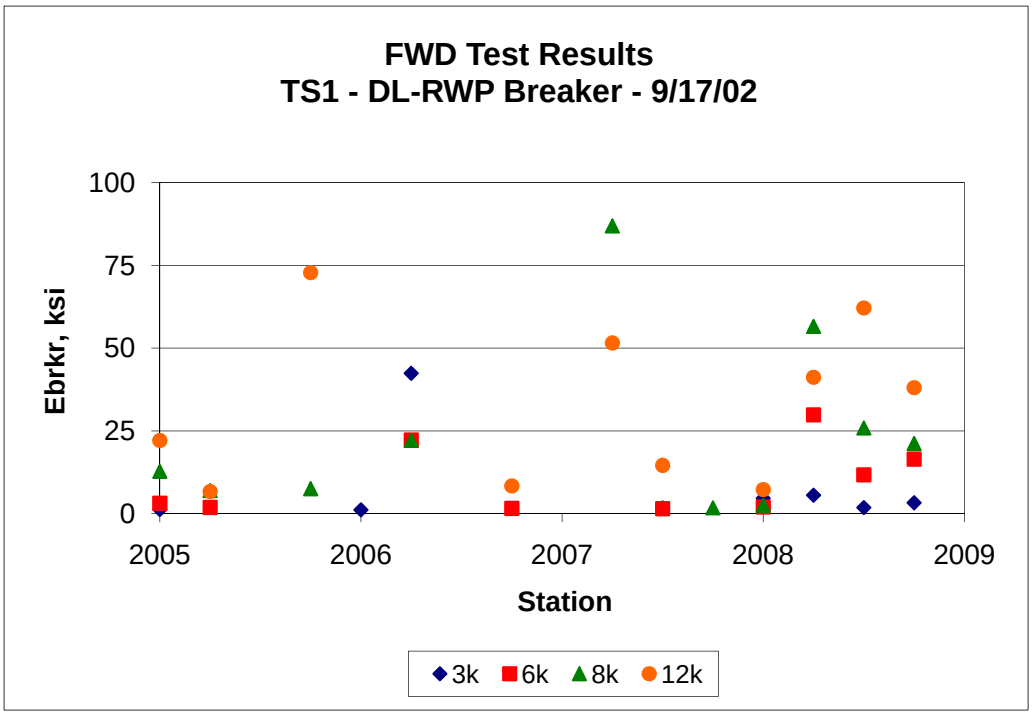

Figure 7: Rescaled Effective Moduli of Breaker Run Layer

FWD tests were conducted on the surface of the compacted subgrade layer in TS2 between stations 2011+75 to 2018+25. The FWD was positioned only within the right wheel path of the driving lane (DL-RWP) using FWD loads ranging from approximately 4,000 to 17,000 lbs. The effective subgrade modulus at each test location was estimated as the minimum value obtained by the application of Eqn. 2. Figure 8 provides profile plots of the effective subgrade moduli for each test load. As shown, there is a general tendency of increased subgrade modulus with increasing test station. This effect may be correlated with a cut/fill transition which occurred between stations 2008+00 to 2020 + 00. There also appears to be a trend of decreasing modulus with increased load level, typical of stress-softening fine-grained soils; however, this trend is erratic and in many cases very small.

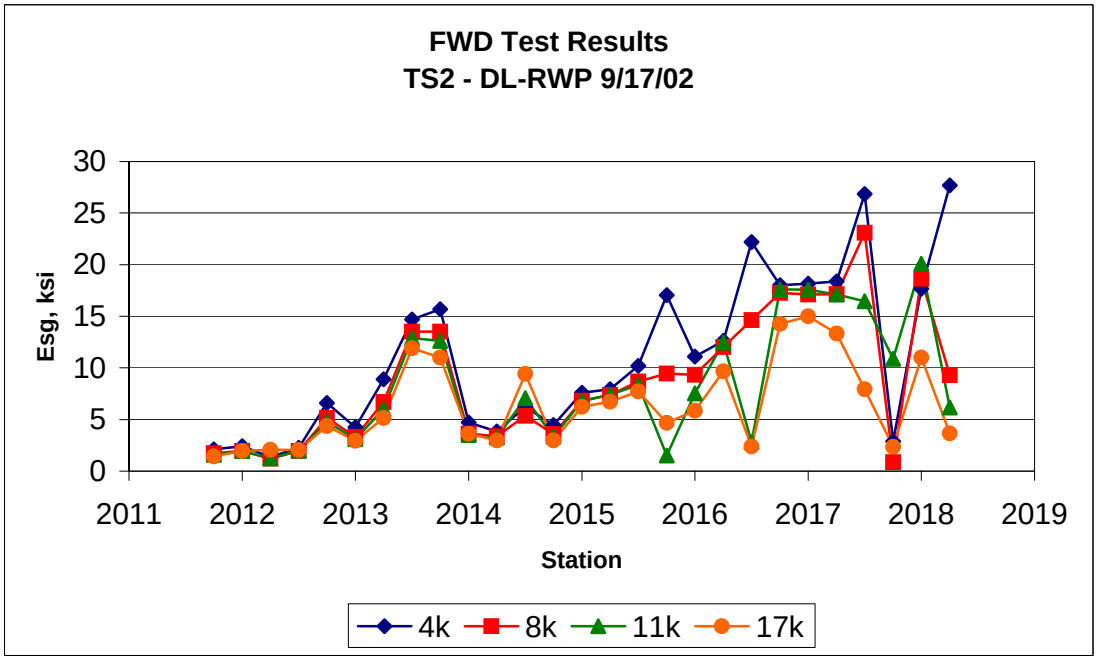

Figure 8: Effective Subgrade Moduli in TS2

2.2 Pre-Paving FWD Testing – Sept 18, 2002

A second round of pre-paving FWD tests was conducted on September 18th within TS1 & TS2. These tests were conducted essentially after all grading and compaction operations were complete and prior to the application of dense graded base course materials. Tests in TS1 were conducted between stations 2004+00 to 2010+75. The FWD was positioned within the right wheel path of the driving lane (DL-RWP) and the center of the passing lane (PL-CEN). Tests were conducted using FWD loads ranging from approximately 3,000 to 15,000 lbs. Equations 2 to 4 were again used to estimate the moduli of the subgrade and breaker run materials. Figures 9 and 10 provide profile plots of the estimated subgrade moduli from each test loading. Figures 11 and 12 provide plots of the estimated breaker run moduli from each test loading. Figures 13 and 14 provide comparative plots of subgrade and breaker moduli within each test lane using the results of the lowest load value, selected as representing the stress state after the complete pavement system is in place. The individual values and trends are similar to those obtained during the previous day's testing.

Tests in TS2 were conducted between stations 2004+00 to 2010+75. The FWD was positioned within the right wheel path of the driving lane (DL-RWP) and the center of the passing lane (PL-CEN). Tests were conducted using FWD loads ranging from approximately 4,000 to 17,000 lbs. Equations 1 and 2 were again used to estimate the moduli of the subgrade materials. Figures 15 and 16 provide profile plots of the estimated subgrade moduli from each test loading. Figure 17 provides a comparative plot of subgrade modulus within each test lane using the results of the lowest load value, selected as representing the stress state after the complete pavement system is in place. The individual values and trends are similar to those obtained during the previous day's testing.

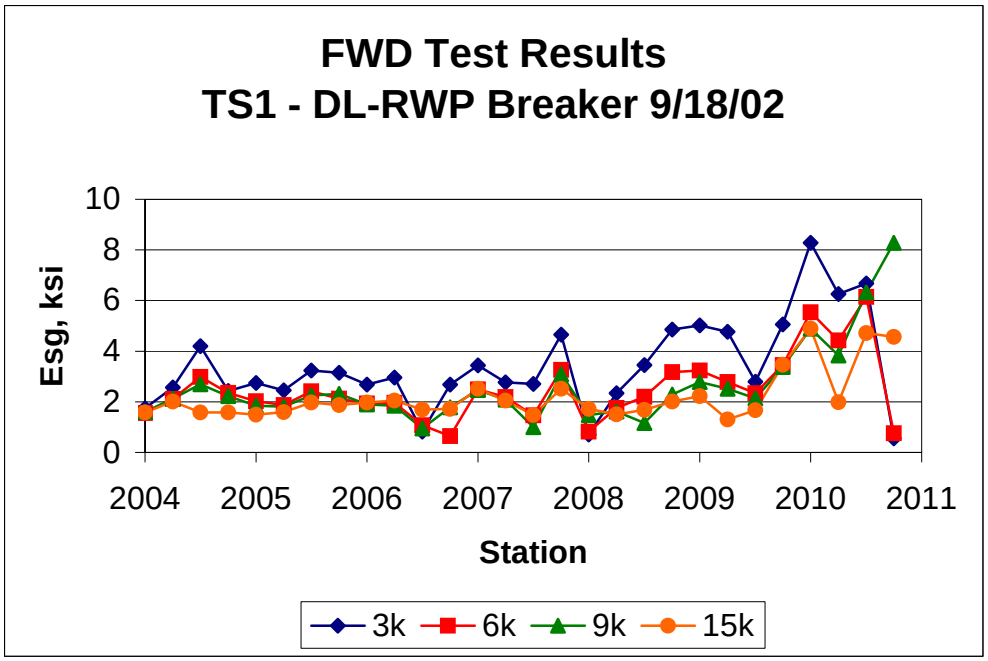

Figure 9: Effective Subgrade Moduli for TS1 Driving Lane Wheelpath

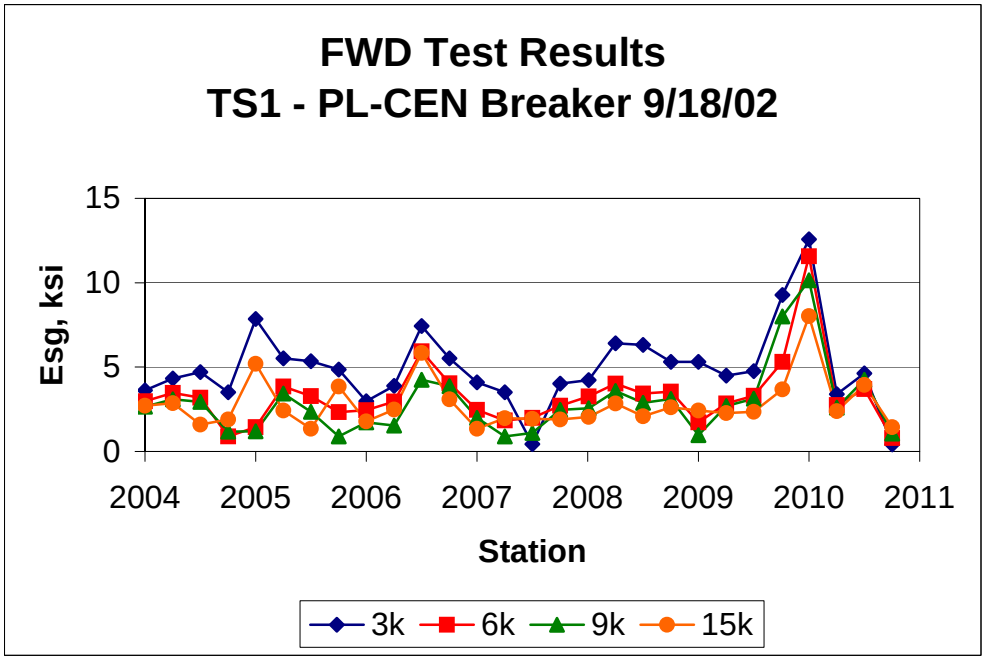

Figure 10: Effective Subgrade Moduli for TS1 Passing Lane Center

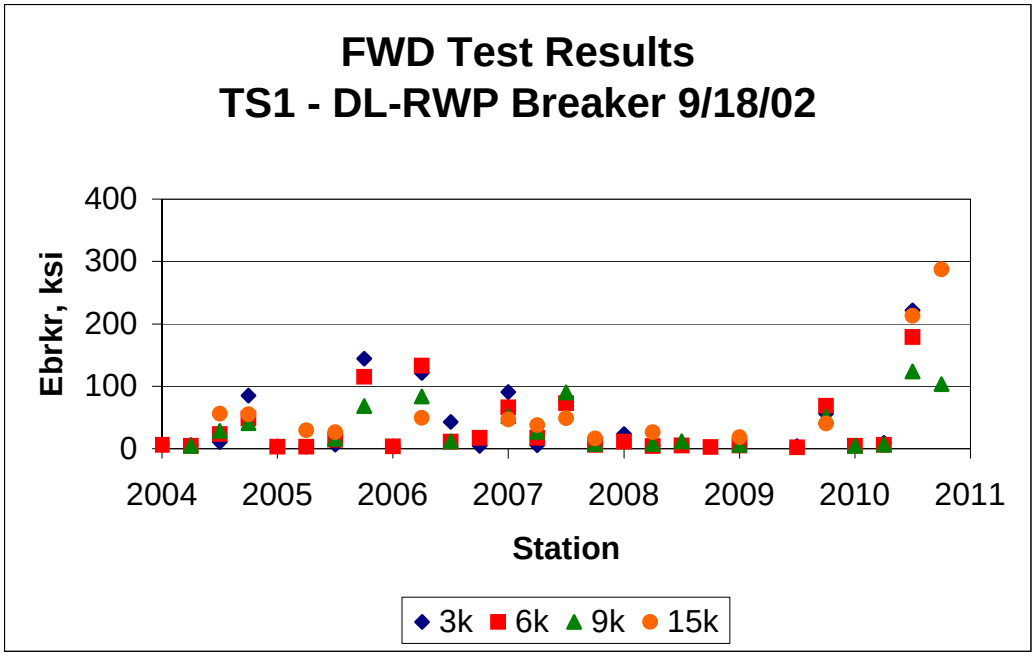

Figure 11: Effective Breaker Run Moduli for TS1 Driving Lane Wheelpath

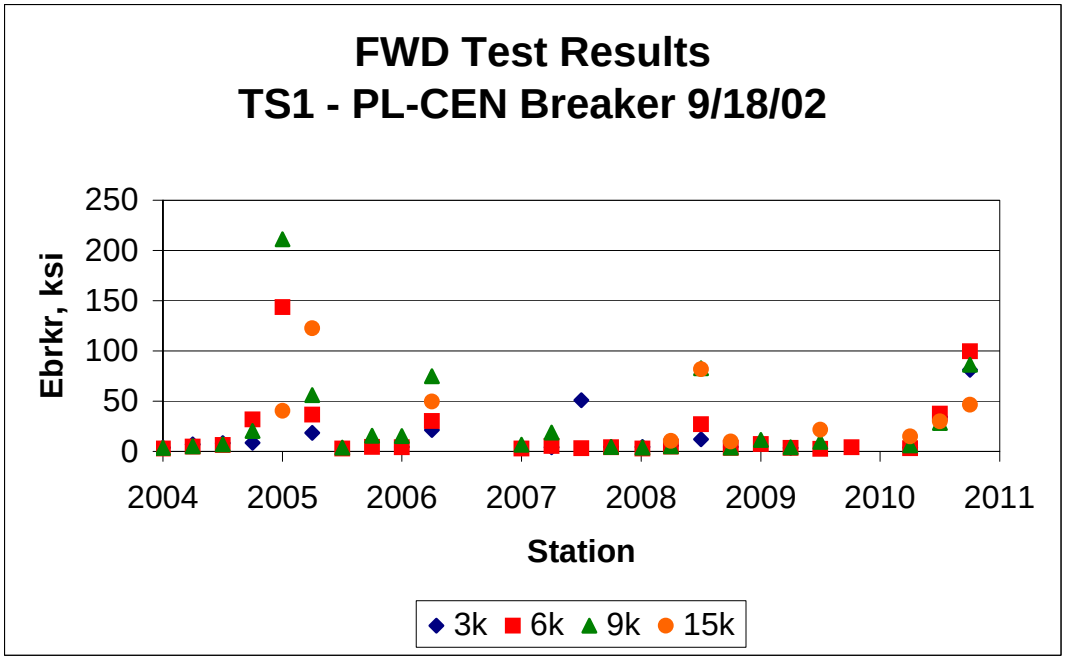

Figure 12: Effective Breaker Run Moduli for TS1 Passing Lane Center

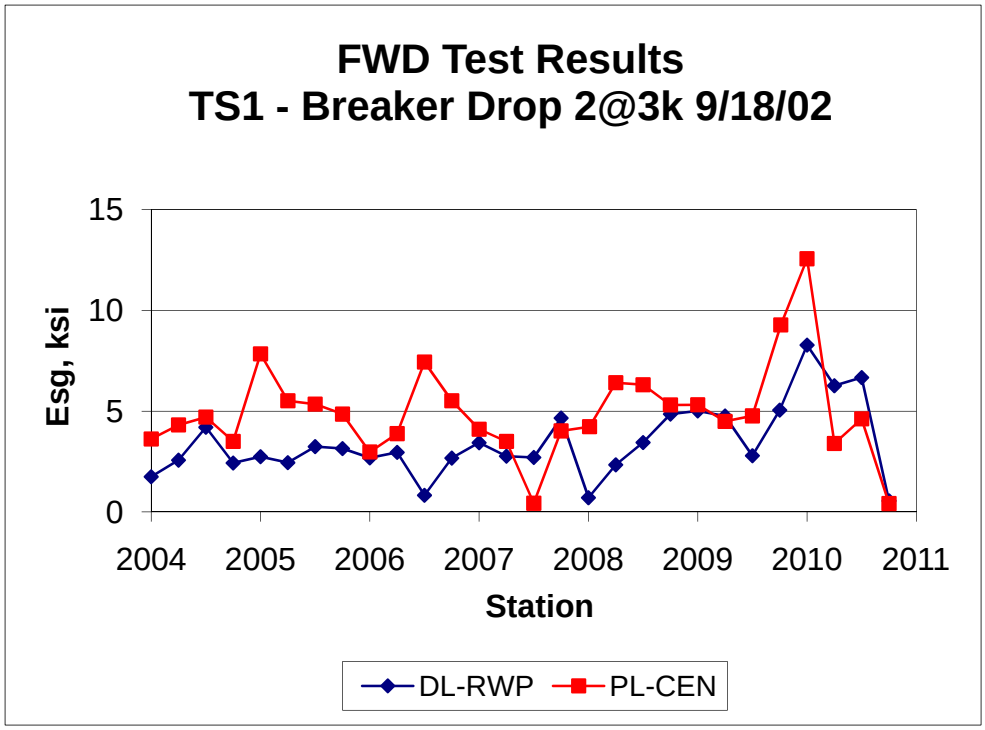

Figure 13: Effective Subgrade Moduli from 3k Load in TS1

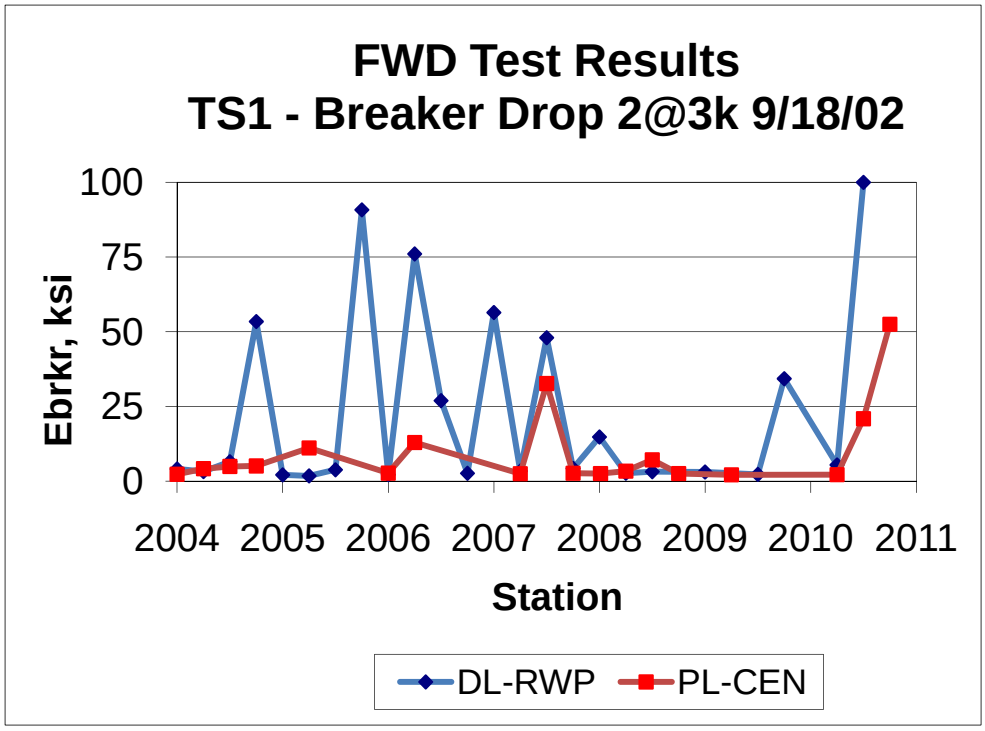

Figure 14: Effective Breaker Run Moduli from 3k Load in TS1

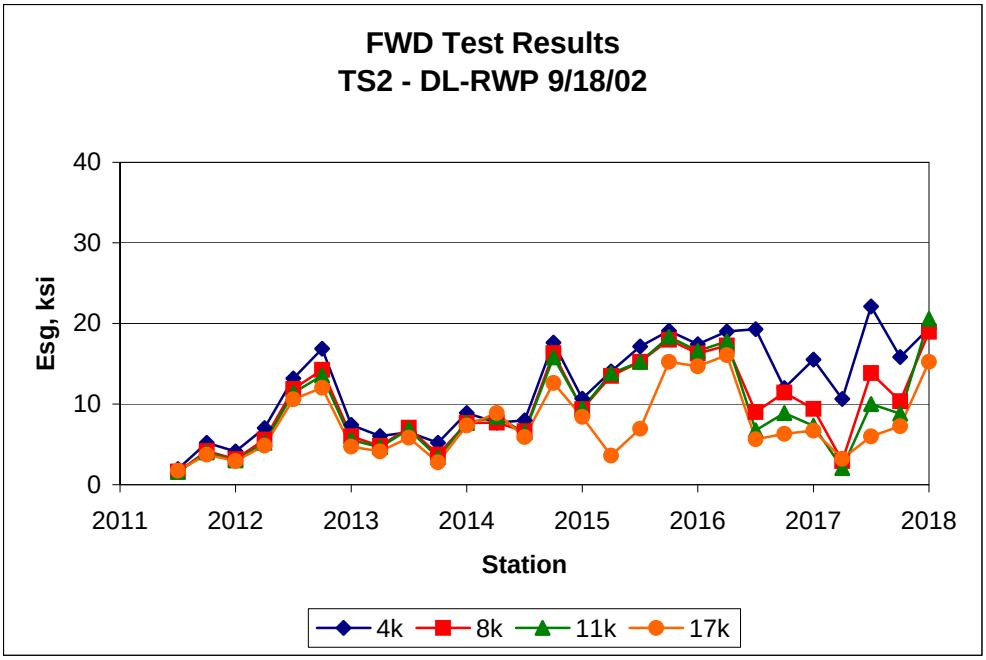

Figure 15: Effective Subgrade Moduli for TS2 Driving Lane Wheelpath

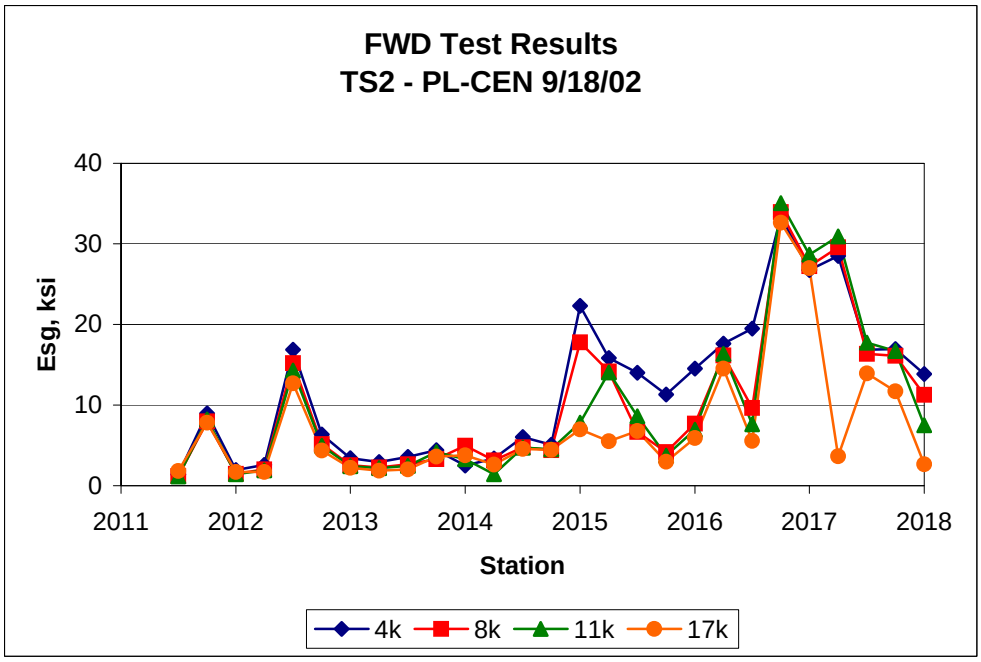

Figure 16: Effective Subgrade Moduli for TS2 Passing Lane Center

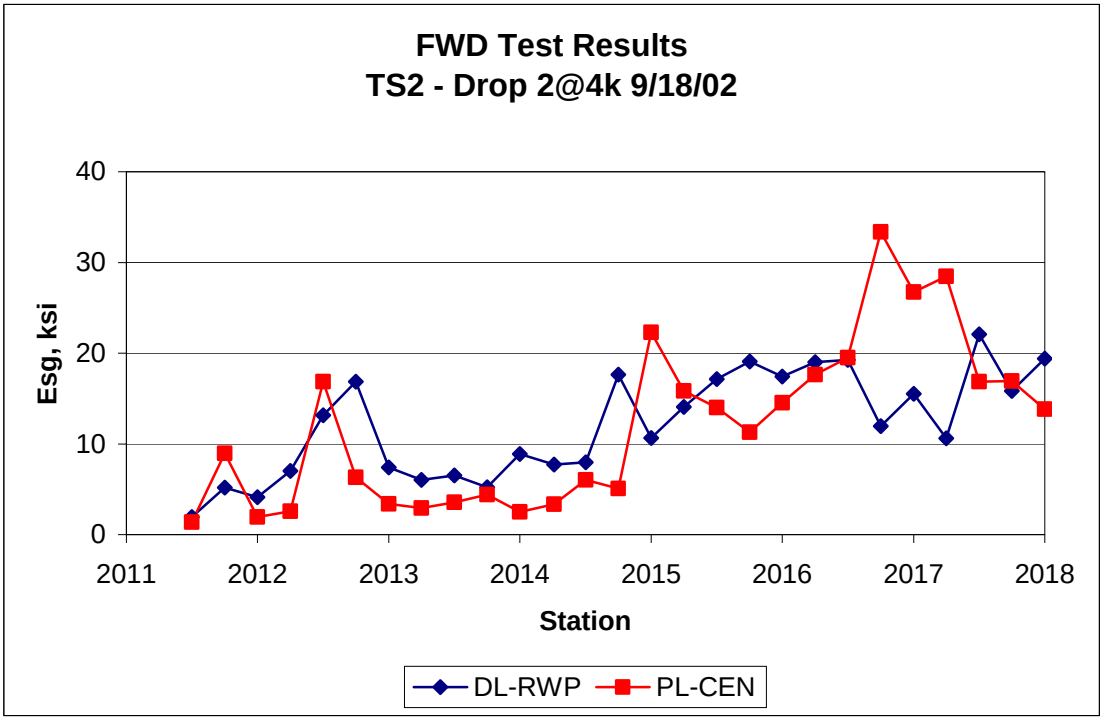

Figure 17: Effective Subgrade Moduli for 3kip Load Drop in TS2

Post-Construction FWD Testing – October 18, 2002

Post-construction FWD testing was conducted within the limits of Test Sections 1 & 2 (TS1, TS2) and the control section (TS3) on October 16, 2002. The FWD was positioned within the center of the driving lane (DL-CEN) at the center of the slab being tested. Tests were conducted using FWD loads ranging from approximately 5,000 to 22,000 lbs. The FWD data was used to backcalculate estimates of the dynamic subgrade support k-value and the elastic modulus of the PCC slabs using incremental deflection analysis techniques developed by Crovetti (2002) combined with average slab thicknesses measured by probing during paving. Figures 18 and 19 provide profile plots of the backcalculated values. As shown, there is general uniformity in the backcalculated results, with the exception of a small group of points near the end of TS2, between stations 2017+24 to 2019+11, which exhibit noticeably higher subgrade k-values and lower Ec values.

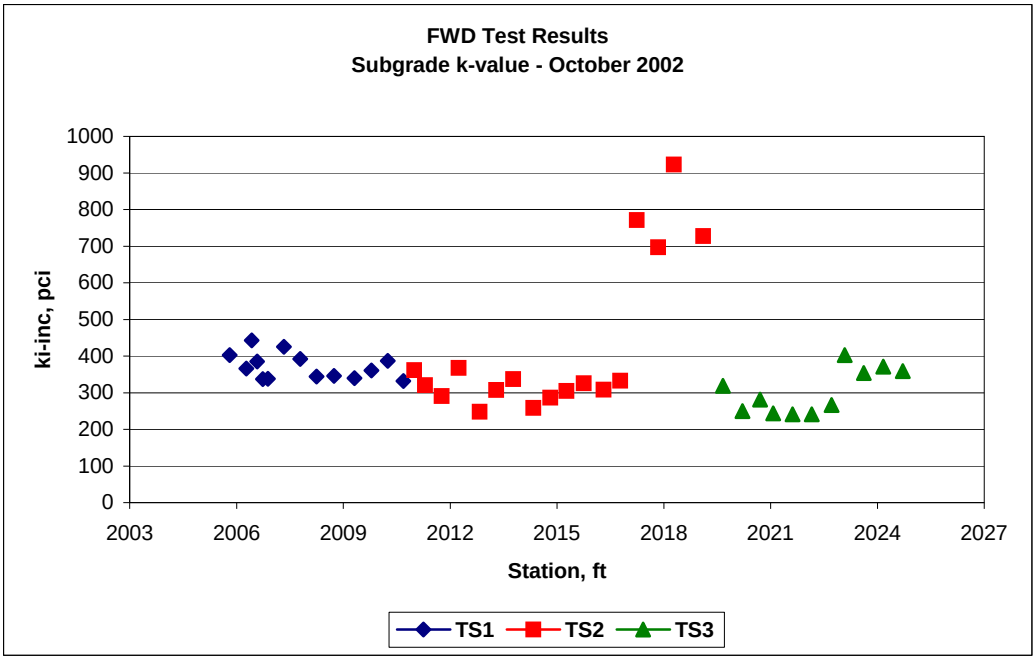

Figure 18: Effective Subgrade k-values from Driving Lane Center Tests

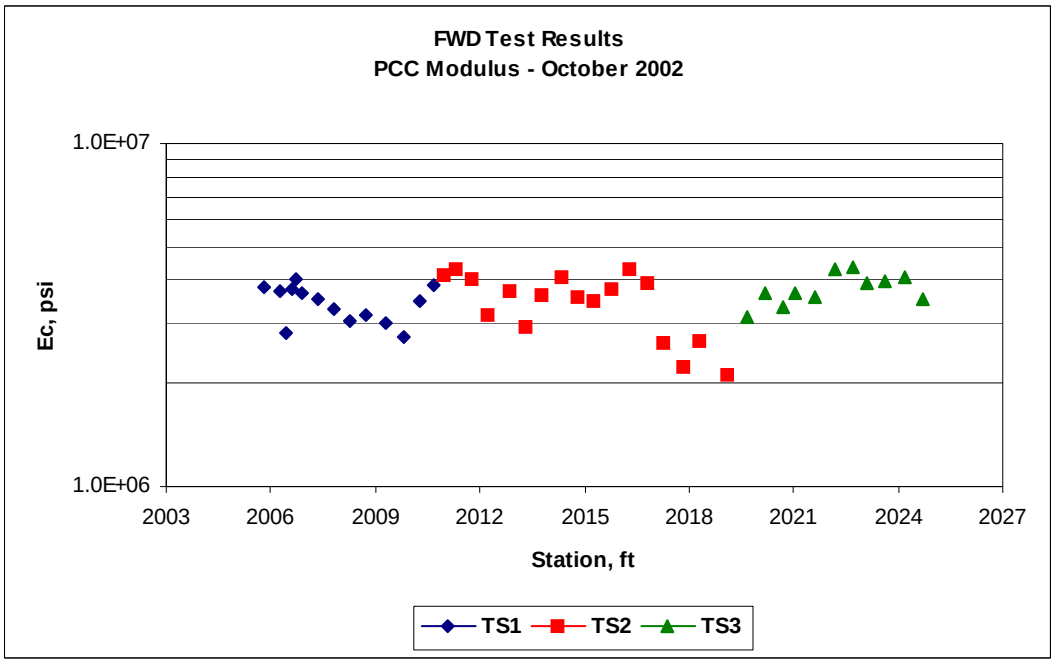

Figure 19: Effective Concrete Moduli from Driving Lane Center Tests

Post-Construction FWD Testing – November 8, 2002

A second round of post-construction FWD testing was conducted within the limits of Test Sections 1 & 2 (TS1, TS2) and the control section (TS3) on November 8, 2002. The FWD was positioned within the center of the driving lane (DL-CEN) at the center of the slab being tested. Tests were conducted using FWD loads ranging from approximately 5,000 to 22,000 lbs. The FWD data was used to backcalculate estimates of the dynamic subgrade support k-value and the elastic modulus of the PCC slabs using incremental deflection analysis techniques developed by Crovetti (2002) combined with average slab thicknesses measured by probing during paving. Figures 20 and 21 provide profile plots of the backcalculated values. As shown, there is general uniformity in the backcalculated results, again with the exception of a small group of points near the end of TS2 and the beginning of TS3, between stations 2017+10 to 2019+45. Here again is the noticeable increase in subgrade k-values but lacking is the noticeable reduction in Ec values.

Post-Construction FWD Testing – April 17-18, 2007

A final round of post-construction FWD testing was conducted within the limits of Test Sections 1 & 2 (TS1, TS2) and the control section (TS3) on April 17-18, 2007. The FWD was positioned within the center of the driving lane (DL-CEN) at the center and transverse joint of the slab being tested and along the outer slab edge at the mid-panel and outer corner positions of the test slab. Compared to previous post-construction testing, additional slab positions were selected for testing (joints, edges and corners) but fewer slabs were tested.

Tests were conducted using FWD loads ranging from approximately 9,000 to 20,000 lbs. The FWD data was used to backcalculate estimates of the dynamic subgrade support k-values (center, edge, corner) and the elastic modulus of the PCC slabs using incremental deflection analysis techniques. Measures of transverse joint and longitudinal edge deflection and load transfer were also computed from the data. Figures 22 and 23 provide profile plots of the backcalculated interior subgrade k-values and slab modulus values (Ec). As shown, there is general uniformity in the backcalculated results. The exception of the small group of points near the end of TS2 and the beginning of TS3, between stations 2017+10 to 2019+45, is not visible in these figures due to the lack of data at these locations. A summary of average results from each test section is provided in Table 1. A review of the data provided in this table indicates numerous anomalies related to TS2 results, most notably joint/corner deflections, longitudinal joint load transfer, and foundation support ratios.

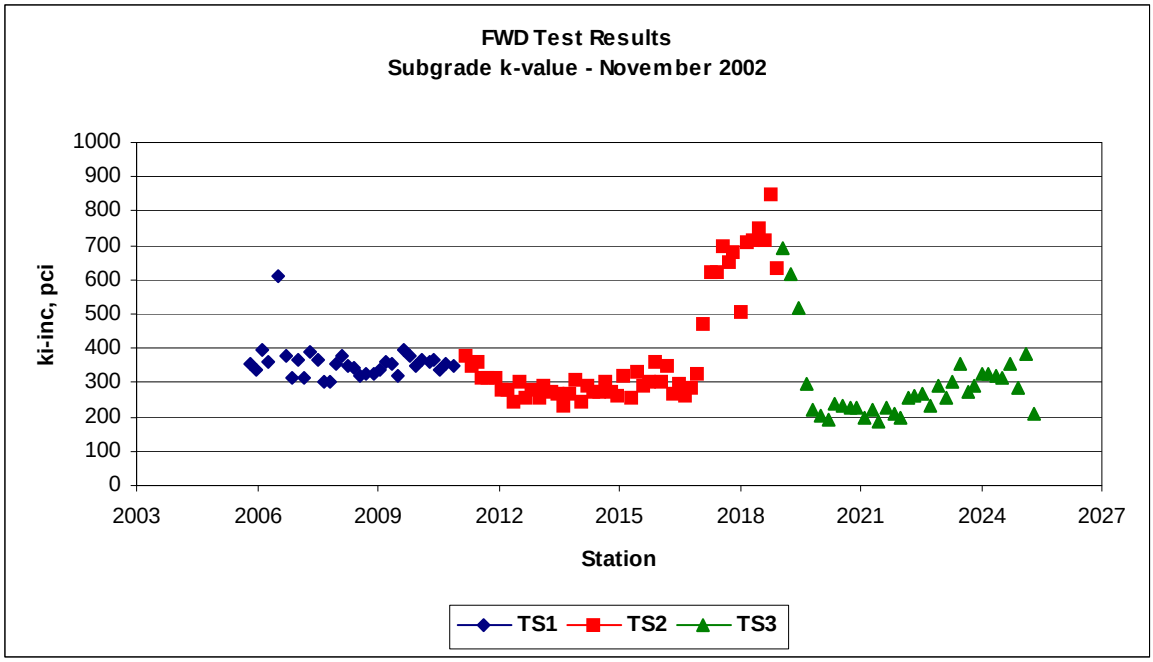

Figure 20: Effective Subgrade k-values from Driving Lane Center Tests

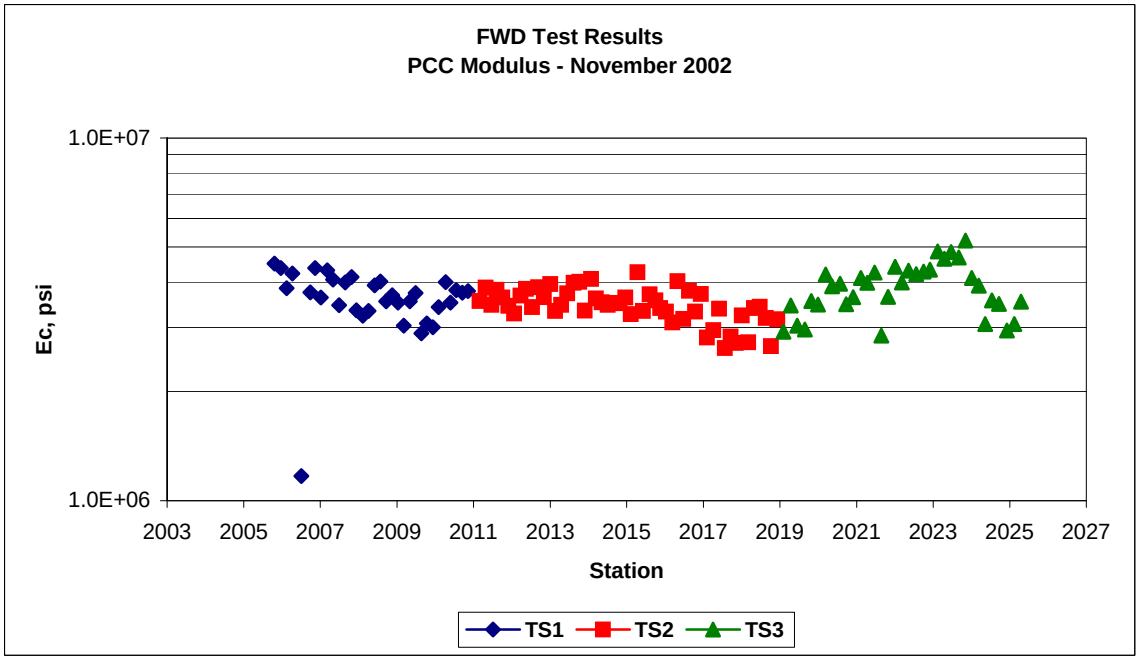

Figure 21: Effective Concrete Moduli from Driving Lane Center Tests

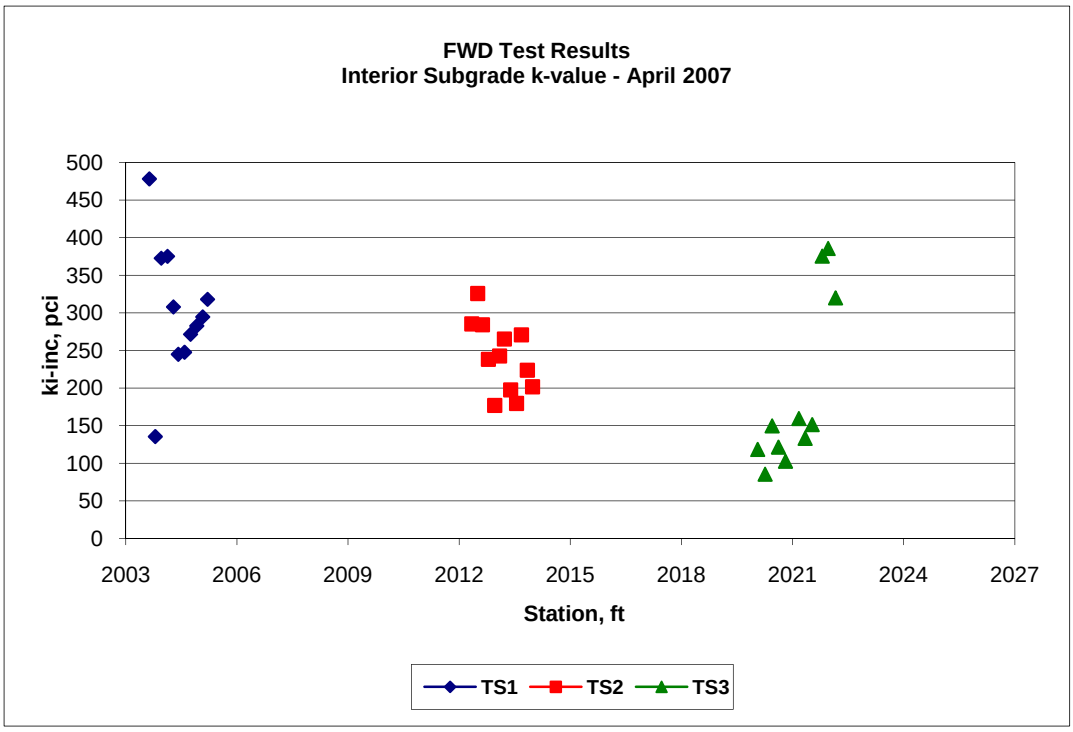

Figure 22: Effective Subgrade k-values from Driving Lane Center Tests

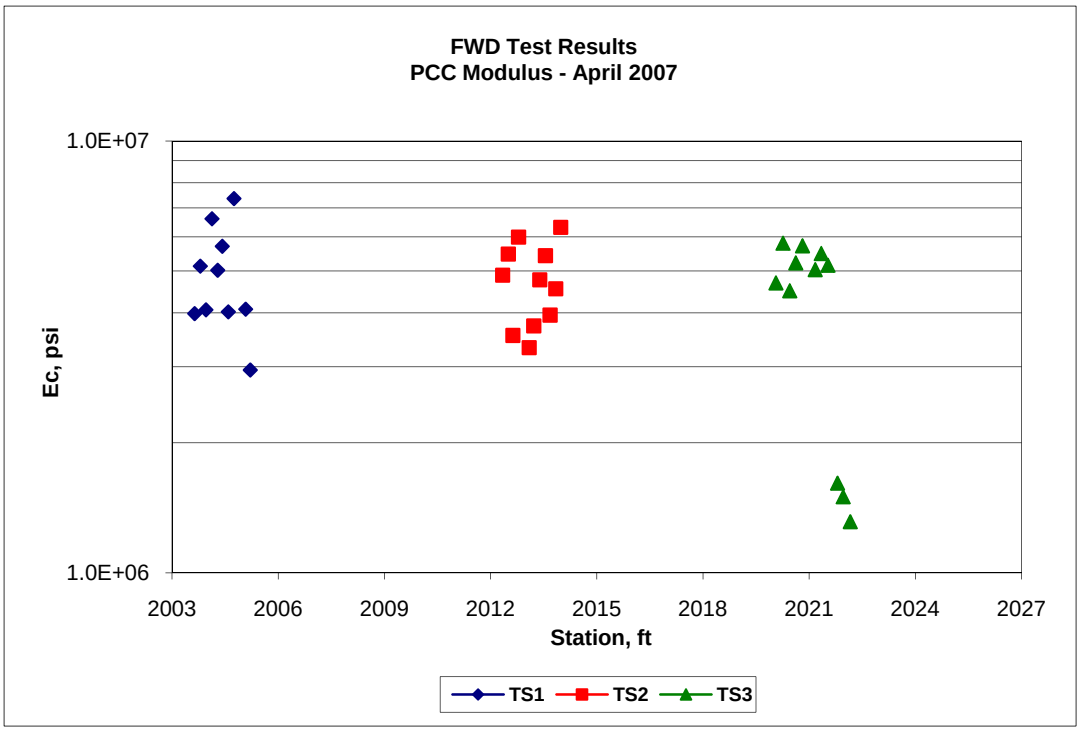

Figure 23: Effective Concrete Moduli from Driving Lane Center Tests

Table 1: Summary of FWD Test Results – April 2007

FWD Test Result	Test Section		
	TS1	TS2	TS3
Average Slab Temperature Gradient (Top-Bottom), F	19.1	9.2 (19.6)	21.8
Interior Dynamic Foundation k-value, pci	303	241 (248)	191
PCC Modulus, psi	5.0E+06	4.8E+06 (4.7)	5.0E+06
Maximum Interior Deflection, mils@9k	2.28	2.33 (2.42)	3.72
Total Approach Transverse Joint Deflection, mils@9k	4.54	6.83 (5.84)	6.64
Total Leave Transverse Joint Deflection, mils@9k	4.60	6.77 (5.63)	6.27
Total Longitudinal Edge Joint Deflection, mils@9k	6.29	8.00 (6.56)	8.96
Total Approach Corner Deflection, mils@9k	11.24	22.79 (15.31)	18.29
Leave Side Transverse Joint Deflection Load Transfer, %	93.8%	95.1% (96.4%)	94.5%
Approach Side Transverse Joint Deflection Load Transfer, %	92.8%	93.4% (94.4%)	91.2%
Longitudinal Edge Joint Deflection Load Transfer, %	89.9%	35.3% (54.4%)	66.1%
Approach Corner Longitudinal Joint Deflection Load Transfer, %	75.7%	19.7% (47.8%)	60.8%
Approach Corner Transverse Joint Deflection Load Transfer, %	92.3%	86.8% (93.7%)	71.7%
Leave Side Transverse Joint Foundation Support k-Value, pci	413	215 (257)	384
Approach Side Transverse Joint Foundation Support k-Value, pci	444	225 (306)	346
Longitudinal Joint Foundation Support k-Value, pci	259	165 (232)	229
Approach Side Corner Foundation Support k-Value, pci	451	160 (278)	343
Leave Side Transverse Joint Foundation Support Ratio	1.44	0.89 (1.07)	2.44
Approach Side Transverse Joint Foundation Support Ratio	1.60	1.00 (1.27)	2.17
Longitudinal Joint Foundation Support Ratio	0.98	0.74 (0.89)	1.25
Approach Side Corner Foundation Support Ratio	1.61	0.71 (1.15)	1.84

Note: mils@9k indicates mils of deflection at a load of 9,000 lbs
Values in parenthesis for TS2 represent average results from retests on Slab 1 at a higher temperature gradient of 19.6 F.

The average total deflections measured at the transverse joints, longitudinal joints and approach corners within TS2 are comparable to those measured in TS3, which is surprising considering TS2 has a thicker slab (13.50 vs 12.25 inches) and a tied concrete shoulder (TS3 has an HMA shoulder). It may be postulated that these higher deflections may be the result of upwards slab curling, even though the average temperature differential was measured at +9.2 ^{o}F, which is close to the commonly considered zero-curling value of +10 ^{o}F. For comparative purposes, reference testing was conducted on one slab within TS2 under a temperature differential of +19.6 ^{o}F, which is similar to measures obtained within TS1 and TS3. FWD results from these comparative tests are provided in parenthesis within Table 1. As shown, the total joint/corner deflections within TS2 at this elevated temperature are markedly reduced, now falling in-between the results from TS1 and TS3. These revised results confirms the benefits of thicker slabs and tied concrete shoulders (TS2 vs TS3) as well as improved subgrade (TS1 vs TS2) on joint/corner deflection response.

The average longitudinal joint deflection load transfers measured in TS2 are also surprising low (35.3% & 19.7% with DT=9.2F and 54.4% & 47.8% with DT=19.2F). Normal values in excess of 70% would be expected for tied concrete shoulders. The foundation support ratios in TS2 are also low in comparison to the other sections, particularly for the DT=9.2F results.

ANALYSIS OF PROJECTED PAVEMENT PERFORMANCE

Long-term performance for jointed concrete pavements is commonly measured in terms of accumulated slab cracking, joint faulting and ride quality. The pavement sections constructed on I-90 were analyzed using both the Mechanistic-Empirical Design Guide (MEPDG) Software v1.0 and the finite element analysis program KENSLABS.

MEPDG v 1.0 Performance Analysis

The MEPDG performance analysis requires the input of site-specific values for traffic, materials and environment. To support this analysis, weigh-in-motion (WIM) data from the I-90 station near Tomah was analyzed to develop representative axle loading spectra. Materials data was obtained from test reports provided by WisDOT and from the results of the FWD tests described previously. Environmental data contained within the MEPDG software for La Crosse, WI was utilized for this analysis.

Traffic Analysis

A detailed truck traffic analysis was completed using design information presented on project plan sheets and worksheets and from WIM data supplied from Station 410253 along I-90 near Tomah. Table 2 provides traffic data provided on the project title sheet and additional derived traffic input values. Table 3 provides vehicle class distributions obtained from project worksheets. The supplied WIM data from 2006-2008 was analyzed to develop representative site-specific factors for axle loading spectra and hourly distributions. Tables 4 through 8 provide pertinent data obtained from the analysis of supplied WIM data.

Table 2: Provided and Derived Traffic Data

Data Provided on Project Title Sheet	
2001 ADT	17,500
2021 ADT	26,500
EB Direction Factor	0.60
% Heavy Trucks	30.2
Design Speed	65 mph
Derived Traffic Inputs	
Average Growth Rate	2.1%
2002 ADT	17,868
2002 ADTT	5,396
Lane Distribution Factor	0.95

Table 3: Vehicle Class Distributions

Vehicle Class	% of Total
Class 4	3.2%
Class 5	8.4%
Class 6	3.1%
Class 7	0.3%
Class 8	8.9%
Class 9	72.5%
Class 10	0.8%
Class 11	2.1%
Class 12	0.6%
Class 13	0.1%

Table 4: Hourly Truck Traffic Distribution

Hour Beginning	% of Total	Hour Beginning	% of Total
Midnight	6.7%	Noon	4.7%
1:00 am	6.0%	1:00 pm	4.7%
2:00 am	6.1%	2:00 pm	4.7%
3:00 am	5.5%	3:00 pm	4.5%
4:00 am	4.0%	4:00 pm	4.5%
5:00 am	2.5%	5:00 pm	4.4%
6:00 am	2.9%	6:00 pm	4.0%
7:00 am	3.3%	7:00 pm	3.7%
8:00 am	3.9%	8:00 pm	3.3%
9:00 am	4.3%	9:00 pm	2.7%
10:00 am	4.7%	10:00 pm	2.3%
11:00 am	4.8%	11:00 pm	1.8%

Table 5: Number of Axles Per Truck

Vehicle Class	**Single Axle**	**Tandem Axle**	**Tridem Axle**	**Quad Axle**
Class 4	1.82	0.18	0.00	0.00
Class 5	2.00	0.00	0.00	0.00
Class 6	1.00	1.00	0.00	0.00
Class 7	1.00	0.00	0.14	0.86
Class 8	3.00	0.00	0.00	0.00
Class 9	1.00	2.00	0.00	0.00
Class 10	1.00	1.00	1.00	0.00
Class 11	5.00	0.00	0.00	0.00
Class 12	4.00	1.00	0.00	0.00
Class 13	3.00	2.00	0.00	0.00

Table 6: Single Axle Load Spectra

Axle Load	Vehicle Class									
	4	5	6	7	8	9	10	11	12	13
3000	2.1%	9.9%	1.5%	0.0%	19.3%	0.1%	0.9%	0.3%	1.1%	1.2%
4000	1.9%	17.1%	2.1%	0.0%	23.9%	1.3%	1.2%	1.3%	1.7%	1.2%
5000	1.9%	17.2%	3.5%	0.0%	17.5%	2.2%	3.9%	1.9%	3.0%	1.3%
6000	3.2%	15.5%	3.7%	0.1%	13.5%	2.6%	1.6%	3.6%	4.3%	1.2%
7000	5.3%	7.8%	3.3%	0.8%	5.2%	2.7%	2.4%	3.3%	4.1%	1.2%
8000	11.0%	7.5%	5.8%	1.9%	4.0%	5.6%	6.3%	7.3%	7.5%	13.5%
9000	10.9%	5.3%	8.5%	3.4%	3.3%	9.6%	8.3%	8.9%	9.6%	7.5%
10000	12.7%	5.2%	13.6%	3.3%	4.0%	20.0%	14.4%	11.5%	11.6%	17.2%
11000	8.8%	3.5%	10.6%	6.1%	2.6%	16.9%	18.3%	9.7%	11.3%	10.8%
12000	10.0%	3.0%	14.7%	3.7%	2.2%	20.4%	16.4%	10.3%	10.5%	24.2%
13000	7.3%	2.0%	10.2%	3.1%	1.0%	11.8%	9.5%	6.7%	7.8%	15.6%
14000	6.8%	2.0%	9.3%	6.4%	0.7%	5.7%	5.9%	9.0%	7.7%	2.3%
15000	5.2%	1.4%	6.9%	6.5%	0.4%	1.0%	4.2%	8.4%	6.1%	1.9%
16000	3.8%	0.9%	2.7%	12.7%	0.3%	0.1%	3.2%	6.0%	4.8%	1.3%
17000	4.0%	0.7%	1.4%	13.1%	0.2%	0.0%	2.2%	5.5%	3.9%	0.0%
18000	2.2%	0.4%	0.8%	11.0%	0.2%	0.0%	1.2%	2.5%	1.7%	0.0%
19000	1.4%	0.2%	0.6%	7.5%	0.1%	0.0%	0.1%	2.2%	1.9%	0.0%
20000	0.6%	0.2%	0.3%	6.6%	0.2%	0.0%	0.0%	0.7%	0.8%	0.0%
21000	0.4%	0.0%	0.1%	4.5%	0.2%	0.0%	0.0%	0.6%	0.3%	0.0%
22000	0.4%	0.1%	0.0%	2.3%	0.2%	0.0%	0.0%	0.2%	0.2%	0.0%
23000	0.1%	0.0%	0.1%	2.8%	0.4%	0.0%	0.0%	0.0%	0.1%	0.0%
24000	0.0%	0.1%	0.0%	0.8%	0.1%	0.0%	0.0%	0.1%	0.1%	0.0%
25000	0.1%	0.0%	0.0%	0.7%	0.1%	0.0%	0.0%	0.0%	0.0%	0.0%
26000	0.0%	0.0%	0.0%	0.2%	0.1%	0.0%	0.0%	0.0%	0.0%	0.0%
27000	0.0%	0.0%	0.0%	0.2%	0.2%	0.0%	0.0%	0.0%	0.0%	0.0%
28000	0.0%	0.0%	0.0%	0.2%	0.0%	0.0%	0.0%	0.0%	0.0%	0.0%
29000	0.0%	0.0%	0.0%	0.3%	0.1%	0.0%	0.0%	0.0%	0.0%	0.0%
30000	0.0%	0.0%	0.0%	0.8%	0.0%	0.0%	0.0%	0.0%	0.0%	0.0%
31000	0.0%	0.0%	0.0%	0.3%	0.0%	0.0%	0.0%	0.0%	0.0%	0.0%
32000	0.0%	0.0%	0.1%	0.2%	0.0%	0.1%	0.0%	0.0%	0.0%	0.0%
33000	0.0%	0.0%	0.0%	0.2%	0.0%	0.0%	0.0%	0.0%	0.0%	0.0%
34000	0.0%	0.0%	0.1%	0.5%	0.1%	0.0%	0.0%	0.0%	0.0%	0.0%
Total	100%	100%	100%	100%	100%	100%	100%	100%	100%	100%

Table 7: Tandem Axle Load Spectra

Axle Load	Vehicle Class						
	4	6	8	9	10	12	13
6000	2.2%	4.1%	11.8%	0.8%	0.2%	0.3%	0.0%
8000	0.2%	5.4%	5.6%	1.5%	0.2%	0.8%	0.0%
10000	1.8%	11.9%	7.8%	3.2%	1.3%	1.3%	0.0%
12000	2.1%	8.7%	7.8%	4.8%	3.1%	2.3%	0.0%
14000	3.9%	7.7%	8.1%	5.8%	4.5%	6.9%	0.0%
16000	3.5%	7.0%	8.1%	6.1%	4.5%	7.5%	0.0%
18000	2.6%	8.7%	8.3%	5.8%	4.4%	11.7%	0.0%
20000	3.7%	6.3%	7.5%	6.2%	6.2%	12.7%	0.0%
22000	3.5%	7.6%	5.6%	6.1%	7.2%	15.9%	0.0%
24000	8.2%	6.5%	5.8%	5.9%	6.8%	14.5%	0.0%
26000	4.7%	6.0%	3.6%	6.2%	7.9%	10.2%	0.0%
28000	12.3%	4.7%	2.6%	8.0%	9.8%	8.3%	0.0%
30000	9.6%	4.8%	2.3%	8.7%	8.0%	2.9%	0.0%
32000	13.5%	3.3%	1.5%	8.6%	11.4%	3.0%	0.0%
34000	8.7%	2.5%	1.2%	7.8%	6.7%	0.8%	0.0%
36000	8.8%	1.2%	1.4%	6.0%	7.0%	0.3%	10.8%
38000	5.3%	1.2%	0.4%	3.9%	4.2%	0.6%	10.8%
40000	3.1%	1.3%	0.8%	2.2%	2.4%	0.0%	9.4%
42000	1.7%	0.3%	0.5%	1.2%	2.3%	0.0%	5.9%
44000	0.5%	0.3%	0.2%	0.6%	0.4%	0.0%	5.8%
46000	0.1%	0.2%	0.3%	0.2%	0.4%	0.0%	5.8%
48000	0.0%	0.0%	0.9%	0.1%	0.1%	0.0%	5.8%
50000	0.0%	0.1%	1.6%	0.1%	0.0%	0.0%	5.8%
52000	0.0%	0.0%	1.5%	0.0%	0.0%	0.0%	29.8%
54000	0.0%	0.0%	1.8%	0.0%	0.0%	0.0%	10.1%
56000	0.0%	0.0%	1.2%	0.0%	0.0%	0.0%	0.0%
58000	0.0%	0.0%	0.7%	0.0%	0.0%	0.0%	0.0%
60000	0.0%	0.0%	0.4%	0.0%	0.0%	0.0%	0.0%
62000	0.0%	0.1%	0.2%	0.0%	0.0%	0.0%	0.0%
64000	0.0%	0.0%	0.1%	0.0%	0.0%	0.0%	0.0%
66000	0.0%	0.0%	0.1%	0.0%	0.7%	0.0%	0.0%
68000	0.0%	0.0%	0.0%	0.1%	0.0%	0.0%	0.0%
Total	100%	100%	100%	100%	100%	100%	100%

Table 8: Tridem and Quad Axle Load Spectra

Axle Load	Tridem Axles		Quad Axles
	Vehicle Class		Vehicle Class
	7	10	7
12000	0.0%	8.5%	0.0%
15000	0.0%	7.9%	0.0%
18000	1.5%	5.9%	0.0%
21000	1.7%	4.9%	0.0%
24000	1.4%	3.9%	0.0%
27000	4.2%	5.8%	0.2%
30000	5.0%	8.1%	0.8%
33000	6.2%	8.2%	2.4%
36000	9.7%	8.4%	3.2%
39000	7.5%	8.9%	2.9%
42000	9.4%	7.8%	5.8%
45000	18.1%	6.5%	3.2%
48000	8.2%	6.8%	4.5%
51000	10.7%	2.2%	7.4%
54000	3.5%	1.8%	12.4%
57000	2.4%	1.2%	13.7%
60000	4.7%	1.7%	13.1%
63000	2.9%	0.9%	11.6%
66000	0.7%	0.7%	9.3%
69000	0.3%	0.0%	1.4%
72000	0.3%	0.0%	1.5%
75000	0.3%	0.0%	3.9%
78000	0.3%	0.0%	0.5%
81000	0.3%	0.0%	0.3%
84000	0.3%	0.0%	0.2%
87000	0.5%	0.0%	0.2%
90000	0.0%	0.0%	0.2%
93000	0.0%	0.0%	1.0%
Total	100%	100%	100%

Materials Analysis

Design inputs for the PCC, aggregate and soil materials were developed from a review of the FWD test results, project materials test reports, and collected ride quality data. Table 9 provides a summary of the materials data inputs used for the MEPDG v1.0 analysis.

Table 9: Materials Data Inputs for MEPDG Analysis

Material Input	Test Section		
	TS1	TS2	TS3
PCC Modulus, psi	5.0E+06	4.8E+06	5.0E+06
28-day Compressive Strength, psi	5,027	5,027	6,151
Open Graded Aggregate Modulus, psi	15,000	15,000	15,000
Dense Graded Aggregate Modulus, psi	30,000	30,000	30,000
Breaker Run Modulus, psi	30,000	n.a.	n.a.
Initial IRI, in/mi	83	71	70

MEPDG Performance Outputs

The MEPDG v1.0 program outputs include predictions of accumulated faulting, cracking and roughness. For this analysis, a 60 year design life and 90% design reliability were chosen. Figure 3.1 provides MEPDG faulting predictions for the three test sections. As shown, all sections are expected to perform adequately with 60-year faulting levels projected to be below threshold values of 0.25 inches. The increased PCC thickness in sections TS1 and TS2 are expected to result in reduced faulting compared to section TS3.

Figure 25 provides MEPDG slab cracking predictions for each test section. As shown, TS1 and TS2 are both predicted to have 0% cracking after 60 years at the 50% reliability level and 3.8% cracking at the 90% reliability level. TS3 is predicted to have 28.3% cracking after 60 years at the 50% reliability level and 41.2% slab cracking at the 90% reliability level.

Figure 26 provides MEPDG roughness predictions for each section in terms of IRI values. A secondary comparison was made between MEPDG predicted and field measured IRI values, which were typically obtained during early afternoon hours. Table 10 provides this comparative data. As shown, the field measures are quite erratic for all sections. Furthermore, the short-term MEPDG predicted IRI values are higher than field measures for TS1 & TS2 and relatively close for TS3.

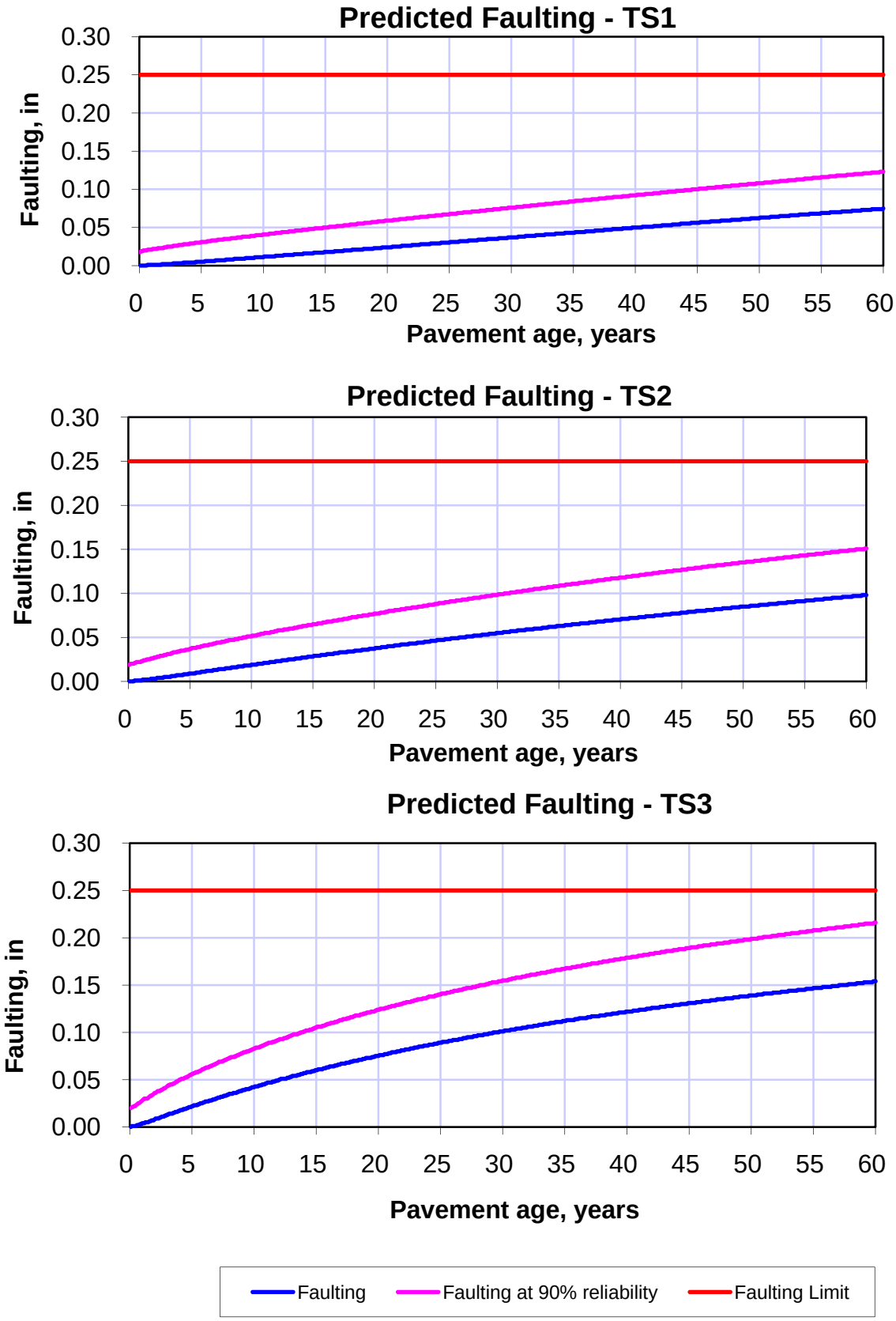

Figure 24: MEPDG Faulting Predictions

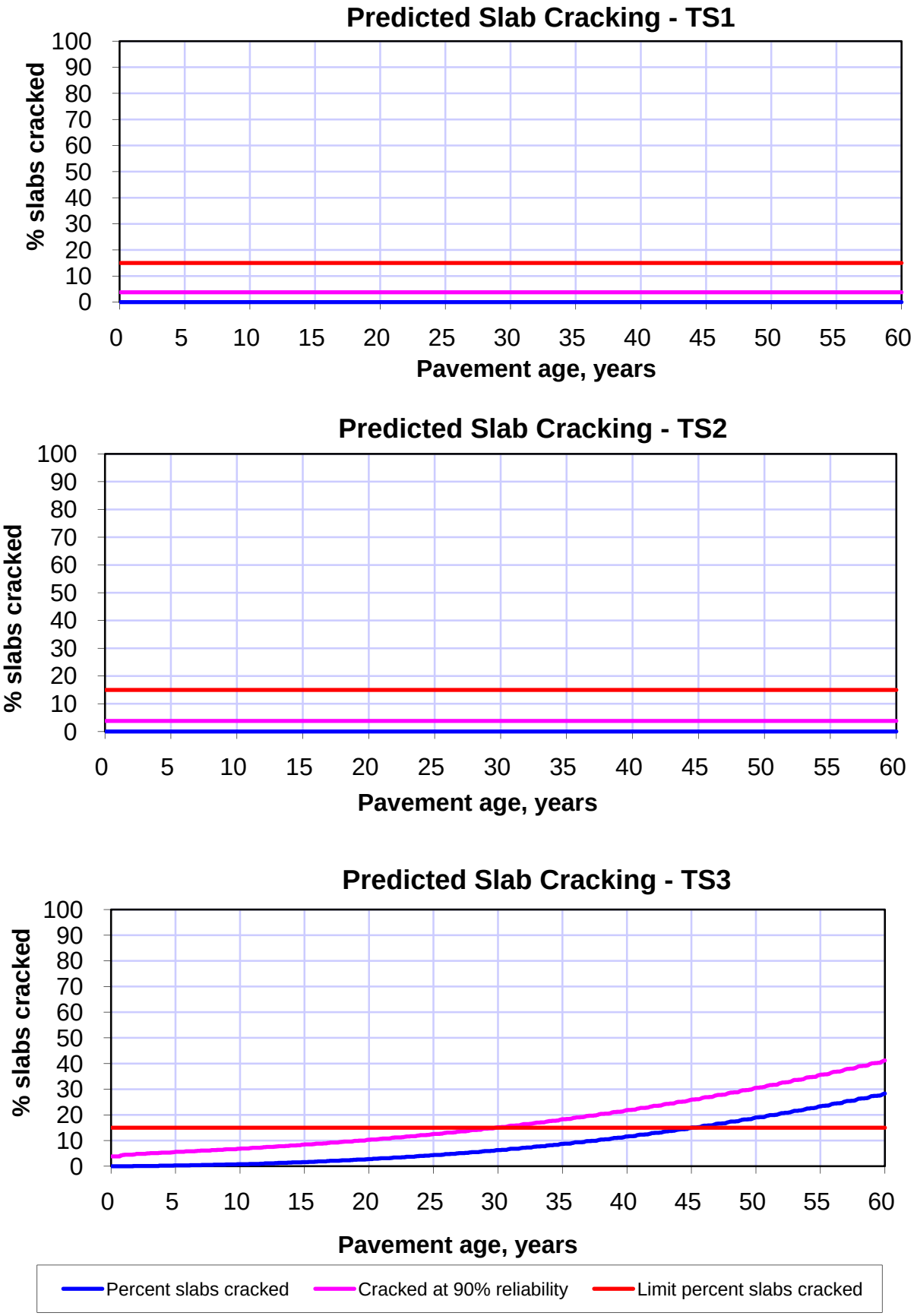

Figure 25: MEPDG Cracking Predictions

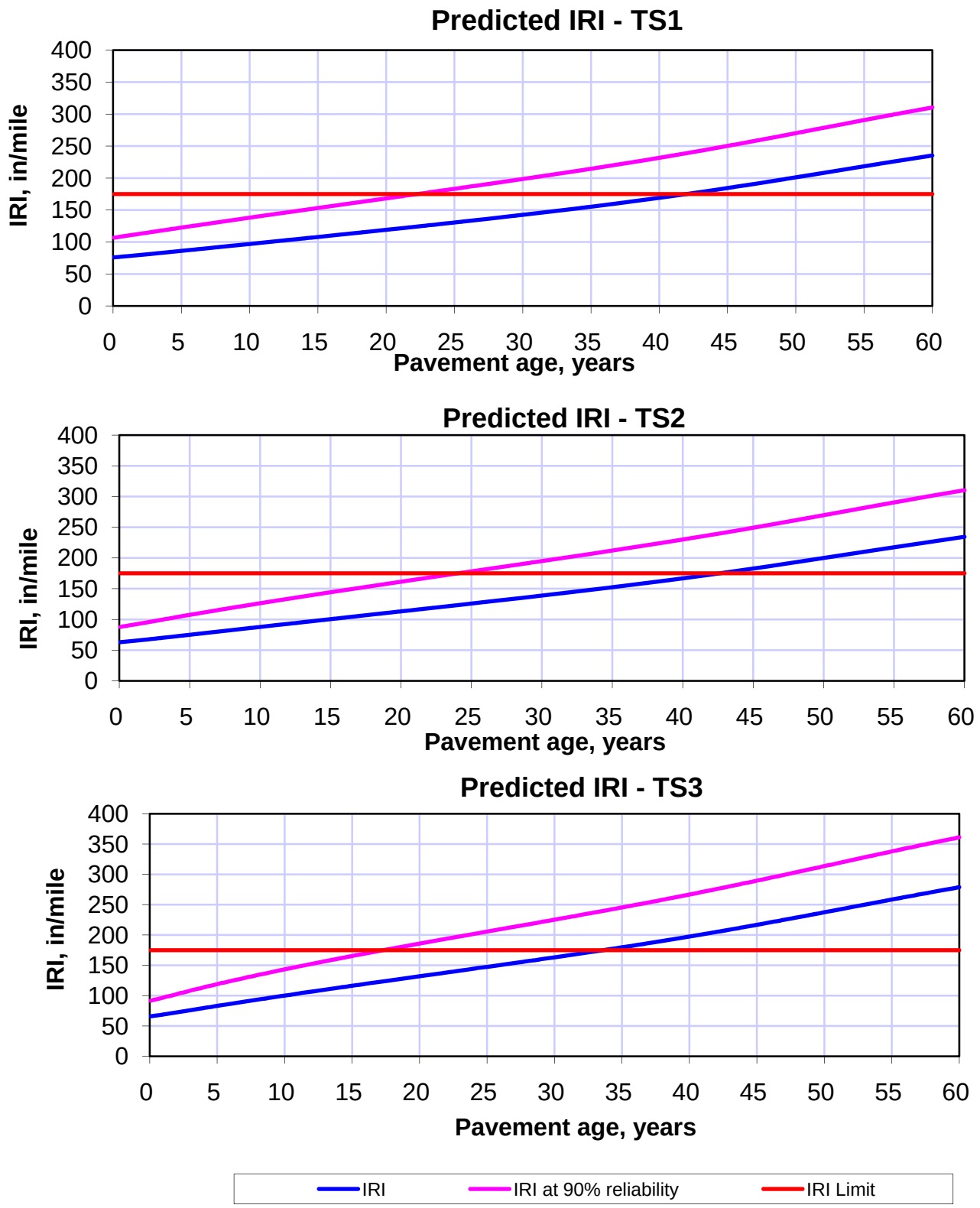

Figure 26: MEPDG IRI Predictions

Table 10: Comparison of Field and MEPDG IRI Values

IRI Date	IRI Time	Accum. Trucks	TS1			TS2			TS3		
				MEPDG			MEPDG			MEPDG	
			Field	50%	90%	Field	50%	90%	Field	50%	90%
9-26-02	6 AM	0	96			80			77		
9-26-02	2 PM	0	87			79			74		
9-27-02	12 PM	0	75			58			59		
9-29-02	2 PM	0	65			52			65		
9-26/29-02	Ave PM	0	76	76	76	63	63	63	66	66	66
8-5-03	8 AM	1,029,790	83	78	110	84	65	91	74	68	96
9-1-04	1 PM	2,270,410	69	80	113	101	67	95	67	72	102
7-5-05	1 PM	3,246,310	71	82	116	71	69	99	78	75	107
8-30-06	1 PM	4,537,530	72	84	119	74	72	103	95	79	113
9-17-07	1 PM	5,857,960	70	86	122	61	75	107	79	83	119
Sep 2010		9,676,300		93	132		83	119		93	134
Sep 2020		24,268,900		114	162		108	154		126	178
Sep 2030		42,232,300		138	192		134	188		157	218
Sep 2040		64,345,300		163	225		161	223		190	258
Sep 2050		91,566,300		194	262		193	261		229	304
Sep 2062		132,654,000		235	310		234	310		279	361
ΔIRI / yr				2.6	3.9		2.8	4.1		3.6	4.9
Years to IRI = 175				41.9	22.2		42.7	24.0		33.7	17.2

FINITE ELEMENT ANALYSIS

A finite element analysis (FEA) was completed to investigate the combined effects of load placement, load configuration, load intensity and temperature curling. For comparative purposes, tire inflation pressures of 100 psi were used for all wheel loadings. Single and tandem axle loadings were modeled as shown in Figure 27. Single axle loadings were varied from 3,000 to 14,000 lbs. and tandem axle loadings were varied from 6,000 to 40,000 lbs. These load ranges represent the typical spectra for the dominant Class 5, 8 and 9 truck traffic (See Tables 3, 6 & 7). Axles were positioned with the outer wheel edge located at distances ranging from 0 to 24 inches from the outer slab edge, as illustrated in Figure 28.

Temperature curling values, as indicated by the top of slab minus bottom of slab temperatures, were assumed to vary from -10 to +25 ^{o}F throughout the day. For the FEA, a flat slab condition (full support) was assumed for the +10 ^{o}F temperature difference, which accounts for a built-in slab warp due to variable slab moisture conditions during curing. The percentage of truck traffic assumed during each temperature difference are shown in Table 11. These values were developed based on the hourly truck traffic distribution data provided in Table 4.

.

Table 11: Truck Traffic Distributions During Slab Curling Regimes

Temperature Difference Top – Bottom, ^{o}F Field (FEA)	Percentage of Truck Traffic	Comment
-10 (-20)	10	Upwards slab curling typically occurring between dusk and early morning
-5 (-15)	15	
0 (-10)	25	
5 (-5)	10	
10 (0)	10	Flat slab condition typically occurring during early morning and late afternoon
15 (5)	10	Downwards slab curling typically occurring late-morning to late-afternoon
20 (10)	10	
25 (15)	10	

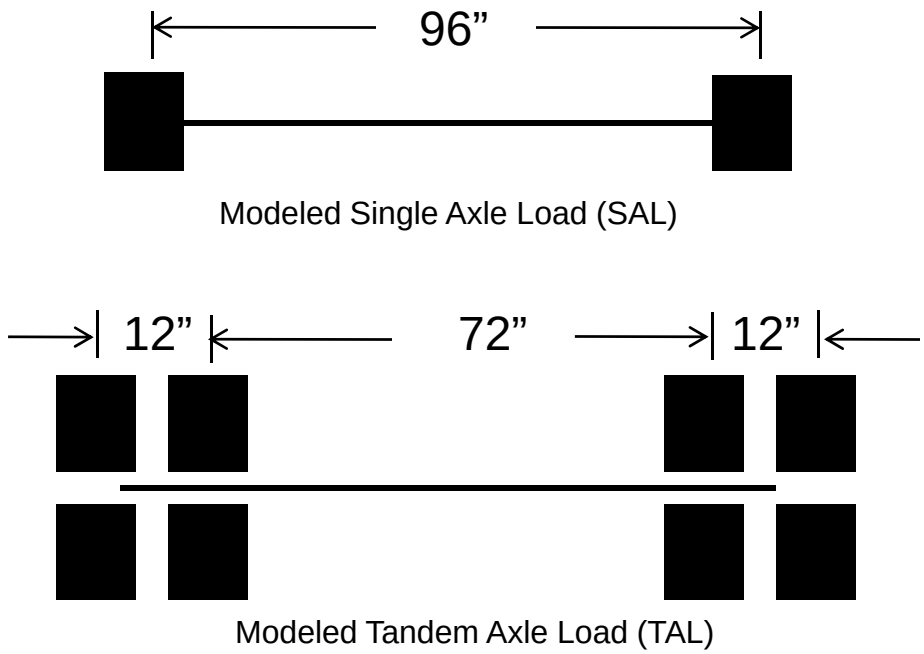

Figure 27: Modeled Axle Loading Used for Finite Element Analysis

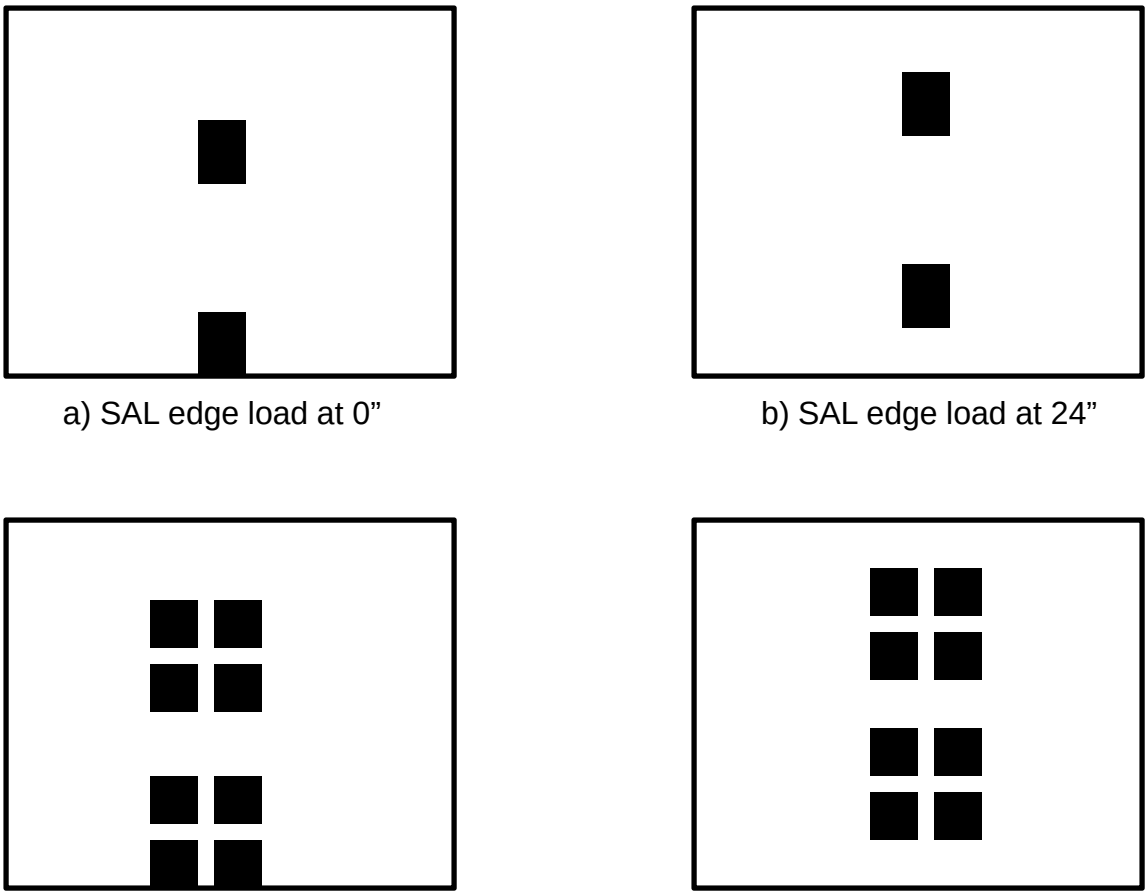

Figure 28: Modeled Edge Loading Placements Used for Finite Element Analysis

Figure 29 schematically illustrates critical loading conditions for upward and downward slab curling conditions. When there is a negative temperature difference (night time), the slab is curled upwards and tension stresses are induced at the top of the slab. This condition can lead to accelerated top-down corner cracking when a wheel load/group is placed near the slab corner (Fig 29a), accelerated mid-panel transverse cracking when two heavy wheel groups are positioned simultaneously near each transverse joint (Fig 29b), and accelerated mid-panel longitudinal cracking when two heavy wheel groups are straddling the mid-panel (Fig 29c). When there is a positive temperature difference (daytime), the slab is curled downwards and tension stresses are induced at the bottom of the slab. This condition can lead to accelerated bottom-up mid-panel transverse cracking when a heavy wheel load/group is positioned near the mid-panel slab edge (Fig 29d). For the mechanistic analysis using FEA results, only the loading conditions illustrated in Figures 29c and 29d were considered, using the load groups/placements illustrated in Figure 28. The load-induced maximum tensile stresses were then used to estimate the expected bottom-up fatigue cracking performance of the constructed test sections.

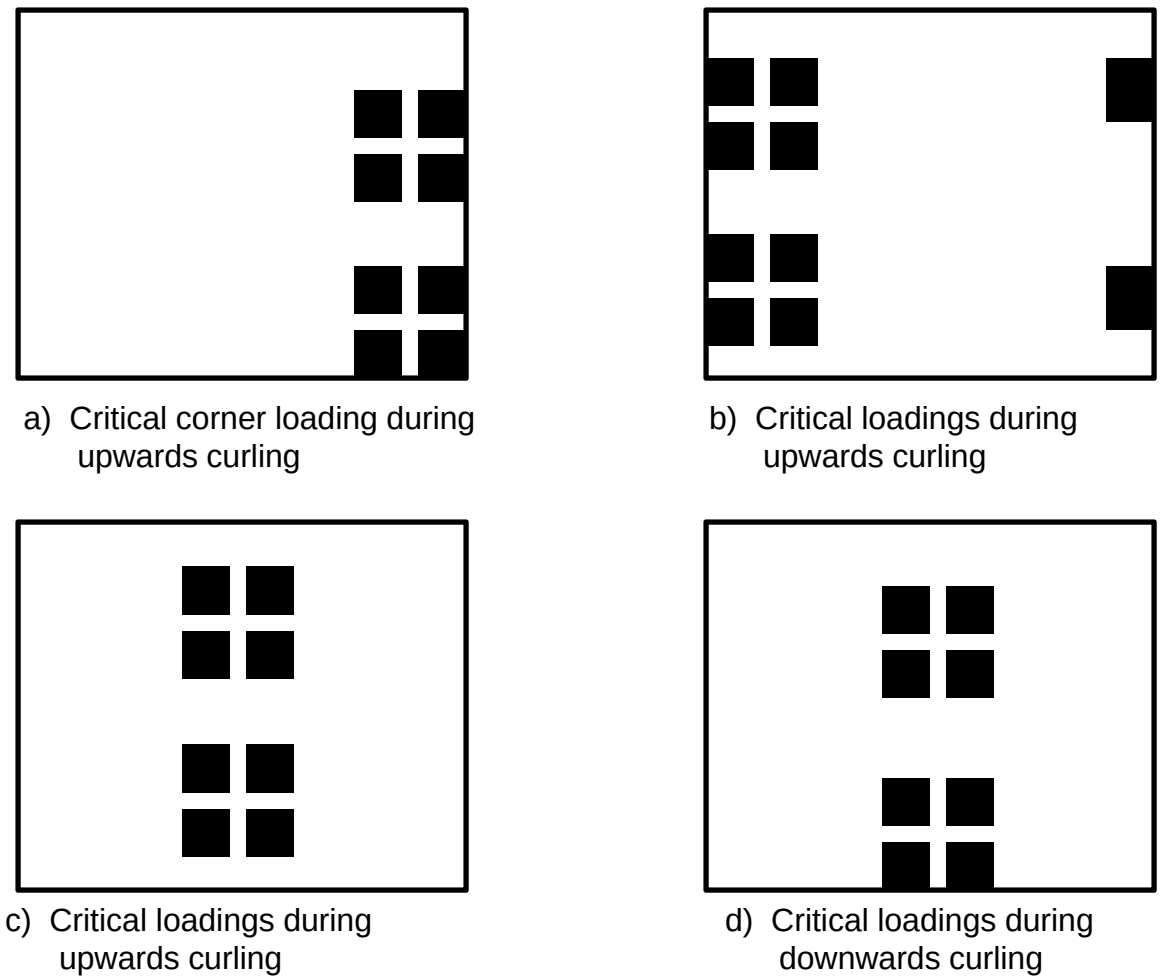

Figure 29: Critical Loadings During Temperature Curling

The analysis properties used for each test section are provided in Table 12. These values were selected based on the results of the FWD testing and were assumed to be representative for the sections throughout the year.

Table 12: Section Properties Used for FEA

Test Section	TS1	TS2	TS3
Slab Thickness, inch	13.5	13.5	12.25
Slab Modulus, psi	5.0 E6	4.8 E6	5.0 E6
Foundation k-value, pci	303	241	191
Radius of Relative Stiffness, inch	43.13	45.21	45.01
Longitudinal Joint Deflection Load Transfer, %	90	35	0

Tables 13 and 14 present the maximum free edge stresses (σ_{FE}) computed for Test Section 1 (TS1) for the range of single axle loads (SAL) and tandem axle loads (TAL), placement locations and slab temperature gradient. Free edge stress represents a condition with no available load transfer across the longitudinal lane-shoulder joint (i.e., HMA shoulder). When a tied concrete shoulder is in place, as is the case in TS1, the working edge stress (σ_E) will be reduced depending on the available load transfer across the longitudinal lane-shoulder joint. Figure 30 illustrates the comparison between stress load transfer and deflection load transfer. FWD testing in TS1 indicates and average longitudinal joint deflection load transfer of approximately 90%, which equates to a stress load transfer of approximately 60%. The working edge stress can be computed as:

$$\sigma_E = \frac{\sigma_{FE}}{1 + LT_\sigma} = F\sigma_{FE} \qquad (5)$$

For TS1, the reduction factor F = 0.63, i.e., the working stresses σ_E would be approximately 63% of the values listed in Tables 13 and 14.

Table 13: Free Edge Stresses Computed with Single Axle Loads for TS1

SAL kips	Edge Distance inch	Slab Temperature Difference (Top – Bottom), °F							
		-20	-15	-10	-5	0	5	10	15
3	0				0.0	30.6	62.3	94.1	125.9
3	12				0.0	17.8	49.5	81.2	112.9
3	24				0.0	15.7	47.8	79.9	112.0
6	0			0.0	23.7	55.5	87.3	119.1	150.9
6	12			0.0	1.4	33.1	64.8	96.5	128.2
6	24				0.0	29.7	61.8	93.8	125.9
9	0		0.0	13.9	45.7	77.5	109.3	141.1	172.9
9	12			0.0	15.4	47.1	78.8	110.5	142.2
9	24			0.0	11.6	43.7	75.8	107.8	139.9
12	0	0.0	2.6	34.4	66.2	98.0	129.8	161.6	193.4
12	12			0.0	28.7	60.4	92.1	123.8	155.6
12	24			0.0	1.4	57.3	64.8	96.5	128.2
14	0	0.0	15.5	47.3	79.1	110.8	142.6	174.4	206.2
14	12		0.0	5.6	37.5	69.4	101.2	133.1	164.9
14	24		0.0	1.8	33.9	66.0	98.1	130.2	162.2

Table 14: Free Edge Stresses Computed with Tandem Axle Loads for TS1

TAL kips	Edge Distance inch	Slab Temperature Difference (Top – Bottom), °F							
		-20	-15	-10	-5	0	5	10	15
6	0				0.0	19.3	46.8	74.4	107.3
6	12				0.0	12.5	40.1	73.9	107.7
6	24				0.0	11.4	40.1	74.0	107.9
10	0			0.0	3.9	31.4	59.0	86.6	114.1
10	12				0.0	20.6	48.2	77.9	111.8
10	24				0.0	18.9	47.5	78.2	112.0
20	0		0.0	5.0	32.6	60.1	87.7	115.3	142.8
20	12			0.0	12.3	39.9	67.6	95.5	123.8
20	24			0.0	9.4	37.4	65.8	94.4	123.0
30	0	0.0	4.2	31.7	59.3	86.9	114.4	142.0	169.6
30	12		0.0	4.3	32.0	59.8	87.5	115.3	143.0
30	24				0.0	56.4	40.1	73.9	107.7
40	0	1.5	29.0	56.5	84.2	111.7	139.3	166.9	194.4
40	12		0.0	23.6	51.4	79.1	106.9	134.6	162.4
40	24		0.0	19.2	47.1	75.1	103.0	131.0	158.9

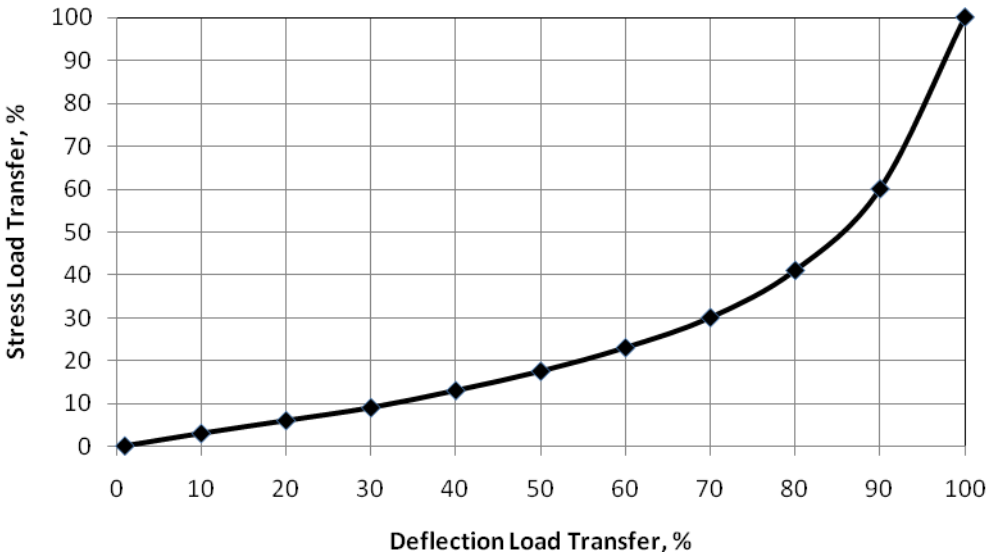

Figure 30: Stress Load Transfer vs Deflection Load Transfer

A limited FEA was completed for Test Sections 2 and 3 to develop relationships between these sections and TS1. For this analysis, the predominant 12-kip SAL and 30-kip TAL were applied over the full range of slab temperature difference for the extreme edge loading case (i.e., edge placement = 0 inches). Figures 31 and 32 illustrate the free edge stress comparisons for each load configuration. As shown, the free edge stresses computed for TS1 and TS2 are similar. The reduced foundation support in TS2 results in lower free edge stresses at elevated slab temperature differentials (downwards curling) and increased stresses at extreme negative temperature differentials (upwards curling). Furthermore, the free edge stresses in TS3 are consistently higher than either TS1 or TS2, primarily due to the reduced slab thickness within this section.

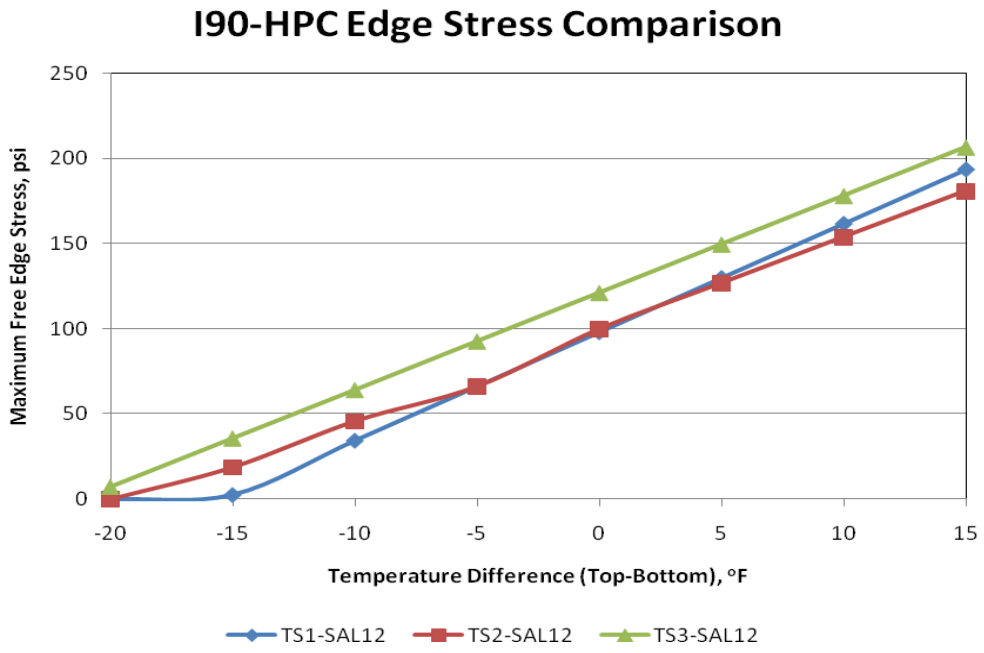

Figure 31: Free Edge Stress Comparison for Single Axle Loadings

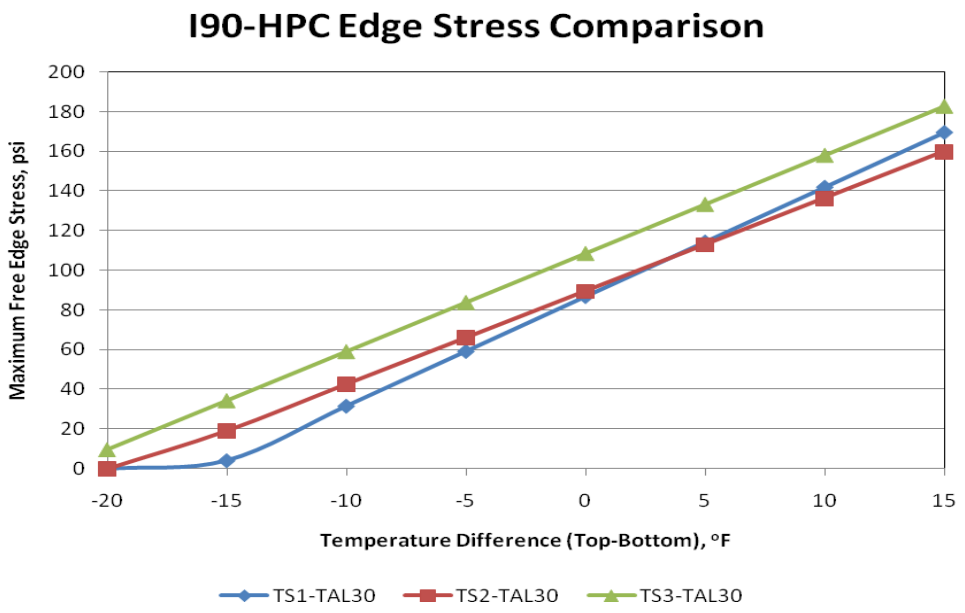

Figure 32: Free Edge Stress Comparison for Tandem Axle Loadings

MECHANISTIC ANALYSIS

The computed working edge stresses (σ_E) can be used to estimate the fatigue life of a pavement section. For bottom-up transverse slab cracking, the fatigue life is estimated as:

$$LogN_f = 2\left(\frac{MR}{\sigma_E}\right)^{1.22} + 0.4371 \qquad (6)$$

Where N_f = number of load to 50% slab cracking
MR = Slab Modulus of Rupture, psi

For this analysis, the slab modulus of rupture was computed based on the backcalculated slab modulus of elasticity, E_c, using the following:

$$E_c = 57,000\sqrt{f'_c} \qquad (7)$$

$$MR = 6.5\sqrt{f'_c} = \frac{E_c}{8,770} \qquad (8)$$

Equations 5 through 8 were used to compute the allowable number of loads to failure, N_f, for each combination of axle load type, axle loading, edge load placement and slab temperature difference. The actual number of yearly axle load applications, N_{app}, assumed for each combination are provided in Table 15.

The fatigue damage, D, associated with each load combination can be computed as:

$$D = \frac{N_{app}}{N_f} \qquad (9)$$

Where N_{app} = Average yearly applications of each axle type/load and temperature combination based on data provided in Tables 3, 4, 5, 6, 7 and 11

The yearly cumulative fatigue damage is determined as the summation of individual damage values computed with Equation 9. For TS1, the yearly cumulative fatigue damage was computed as 2.3×10^{-9}. The projected pavement service life to 50% bottom-up slab cracking is estimated as the inverse of the yearly cumulative fatigue damage, which is essentially unlimited for TS1. This result is in agreement with the MEPDG prediction of 0% slab cracking after 60 years of service.

Table 15: Yearly Loadings Used for Mechanistic Analysis

Axle Type	Axle Load	Edge Placement Inch	Edge Placement % Occurrence	Slab Temperature Difference (Top – Bottom) °F - % Occurrence							
				-10	-5	0	5	10	15	20	25
				10%	15%	25%	10%	10%	10%	10%	10%
SAL	3	0	20%	8,643	12,965	21,608	8,643	8,643	8,643	8,643	8,643
		12	45%	19,447	29,171	48,618	19,447	19,447	19,447	19,447	19,447
		24	35%	15,126	22,688	37,814	15,126	15,126	15,126	15,126	15,126
	6	0	20%	10,278	15,418	25,696	10,278	10,278	10,278	10,278	10,278
		12	45%	23,126	34,690	57,816	23,126	23,126	23,126	23,126	23,126
		24	35%	17,987	26,981	44,968	17,987	17,987	17,987	17,987	17,987
	9	0	20%	10,950	16,425	27,375	10,950	10,950	10,950	10,950	10,950
		12	45%	24,638	36,956	61,594	24,638	24,638	24,638	24,638	24,638
		24	35%	19,163	28,744	47,906	19,163	19,163	19,163	19,163	19,163
	12	0	20%	19,827	29,740	49,567	19,827	19,827	19,827	19,827	19,827
		12	45%	44,610	66,915	111,526	44,610	44,610	44,610	44,610	44,610
		24	35%	34,697	52,045	86,742	34,697	34,697	34,697	34,697	34,697
	14	0	20%	5,825	8,738	14,564	5,825	5,825	5,825	5,825	5,825
		12	45%	13,107	19,661	32,768	13,107	13,107	13,107	13,107	13,107
		24	35%	10,194	15,292	25,486	10,194	10,194	10,194	10,194	10,194
TAL	6	0	20%	2,628	3,942	6,570	2,628	2,628	2,628	2,628	2,628
		12	45%	5,913	8,870	14,783	5,913	5,913	5,913	5,913	5,913
		24	35%	4,599	6,899	11,498	4,599	4,599	4,599	4,599	4,599
	10	0	20%	10,519	15,779	26,298	10,519	10,519	10,519	10,519	10,519
		12	45%	23,668	35,503	59,171	23,668	23,668	23,668	23,668	23,668
		24	35%	18,409	27,613	46,022	18,409	18,409	18,409	18,409	18,409
	20	0	20%	20,382	30,572	50,954	20,382	20,382	20,382	20,382	20,382
		12	45%	45,859	68,788	114,647	45,859	45,859	45,859	45,859	45,859
		24	35%	35,668	53,502	89,170	35,668	35,668	35,668	35,668	35,668
	30	0	20%	28,601	42,902	71,504	28,601	28,601	28,601	28,601	28,601
		12	45%	64,353	96,530	160,883	64,353	64,353	64,353	64,353	64,353
		24	35%	50,052	75,079	125,131	50,052	50,052	50,052	50,052	50,052
	40	0	20%	7,234	10,851	18,086	7,234	7,234	7,234	7,234	7,234
		12	45%	16,277	24,416	40,693	16,277	16,277	16,277	16,277	16,277
		24	35%	12,660	18,990	31,650	12,660	12,660	12,660	12,660	12,660

For TS2 and TS3, the free edge stresses for each combination of load configuration, load magnitude, load placement and slab temperature differentials were estimated based on the relations exhibited in Figures 31 and 32. For TS2, even though the free edge stresses are similar to TS1, the working edge stresses in TS2 are significantly greater than in TS1 due to the markedly reduced longitudinal lane-shoulder deflection/stress load transfer. The yearly cumulative fatigue damage was estimated as 1.4×10^{-5}, which is four orders of magnitude greater than in TS1. However, there again is a prediction of essentially unlimited projected pavement service life to 50% bottom-up slab cracking. This estimation is again in agreement with the MEPDG prediction of 0% slab cracking after 60 years of service.

For TS3, the working edge stresses are significantly increased due to both the reduced slab thickness and the exclusion of the tied concrete shoulder. It should be noted that the apparent deflection load transfer of 66% (Table 1) is not considered due to the existence of the HMA shoulder. The yearly cumulative fatigue damage in TS1 was estimated as 9.7 E-03, which predicts a pavement service life of 104 years to 50% bottom-up slab cracking. This estimation is in general agreement with the MEPDG 50% reliability prediction of 28% slab cracking after 60 years of service.

SUMMARY AND RECOMMENDATIONS

This report presents the results of field testing and related analysis for the high performance concrete (HPC) and control sections located along I-90 in Monroe County, Wisconsin. Deflection data obtained with the WisDOT Falling Weight Deflectometer (FWD) was used to characterize the pavement materials within each section and to provide inputs for detailed mechanistic-empirical pavement analyses. The FWD data analysis indicated general uniformity within each constructed section, in terms of the concrete slab elastic modulus and foundation support k-value. The doweled transverse contraction joints within each test section are providing adequate load transfer, with measure deflection load transfers in excess of 90% for all sections. The deflection load transfer measured across the longitudinal joint separating the driving lane and the tied concrete shoulder was adequate within TS1 (90%) but significantly reduced within TS2 (35%).

The Mechanistic Empirical Pavement Design Guide (MEPDG) software was used to provide 60-year predictions of pavement performance within each test section. The results indicate all sections should remain below a threshold value of 0.25 inches of transverse joint faulting throughout this period. Furthermore, no slab cracking is predicted within the HPC test sections 1 and 2; however, approximately 25% slab cracking is predicted within the control section (TS3). This increased slab cracking is above the commonly accepted threshold value of 15% slab cracking but below the WisDOT terminal value of 50% slab cracking. The MEPDG software predicts 60-year IRI values above the threshold value of 180 inches per mile for all test sections, predominantly due to predictions of high levels of joint spalling. It is common for MEPDG outputs to predict high levels of joint spalling for all jointed concrete pavements expect those with neoprene compression seals due to the assumption of lodged incompressibles causing high compressive stresses along the joint. Experience in Wisconsin has shown that the unsealed transverse joints on high-speed highways due not accumulate incompressibles, hence the IRI performance for these sections may be significantly better than predicted by the MEPDG software.

Recommendations

The actual performance of the constructed section should be monitored on a regular basis to ensure all performance expectations are met. Particular attention should be placed on the development, or lack thereof, of transverse joint spalling. Furthermore, the reason(s) for the reduced load transfer capacity across the longitudinal lane-shoulder joint within TS2 should be investigated to determine if this result is due to FWD measurement procedures or a design, materials, and/or construction defect.